

國立交通大學

電子工程學系 電子研究所碩士班

碩 士 論 文

無線雙向中繼傳輸之前送策略研究

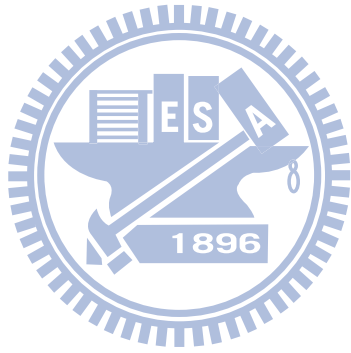


**Study on Forwarding Strategies for Wireless
Bidirectional Relay Transmission**

研 究 生：盧世榮

指 導 教 授：林大衛 博士

中 華 民 國 九 十 九 年 七 月



無線雙向中繼傳輸之前送策略研究

Study on Forwarding Strategies for Wireless Bidirectional Relay Transmission

研究生：盧世榮

Student: Shih-Jung Lu

指導教授：林大衛 博士

Advisor: Dr. David W. Lin

國立交通大學

電子工程學系 電子研究所碩士班



A Thesis

Submitted to Department of Electronics Engineering & Institute of Electronics
College of Electrical and Computer Engineering
National Chiao Tung University
in Partial Fulfillment of the Requirements
for the Degree of
Master of Science
in
Electronics Engineering
July 2010
Hsinchu, Taiwan, Republic of China

中華民國九十九年七月



無線雙向中繼傳輸之前送策略研究

研究生：盧世榮

指導教授：林大衛 博士

國立交通大學

電子工程學系 電子研究所碩士班

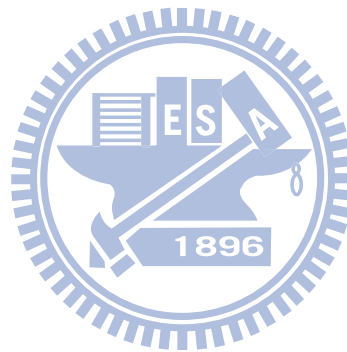
摘要

本篇論文介紹在無線雙向中繼傳輸下的前送策略。在雙向中繼傳輸中，中繼站同時收到由兩端點站傳來的訊號，中繼站接著將收到的混合訊號廣播給兩端點站。利用自身傳送的資料，端點站可以自混合訊號中擷取出預期收到的資料。

在本篇論文中，我們首先簡介中繼傳輸模型以及兩種基本的前送策略：放大前送和解碼前送。接著我們著重於一種以放大前送為基礎而發展出來的前送策略，這種前送策略我們稱之為摺疊前送。我們討論在使用二元調變的折疊前送系統中，中繼站的運作機制以及端點站的資料偵測規則。我們在二維訊號平面進行錯誤率分析，並且將摺疊前送的字元錯誤率表示式由雙重積分化簡為數個單一積分的總和。模擬結果顯示在未編碼的系統中，當通道為對稱狀態時，摺疊前送可以提供比放大前送高 1-1.5 dB 的效能增益。所謂的通道對稱是指兩個端點站與中繼站的鏈結有相同的通道增益。當通道狀態不對稱時，摺疊前送所能提供的效能增益會隨之減少。

接下來我們考慮高次調變的摺疊前送系統。在高次調變的系統中，摺疊前送的運算必須避免解碼模糊的問題。解碼模糊的問題是指端點站利用自身傳送的資

料也無法將對方端點站的資料辨別出來。我們提出使用適當的摺疊閾值來避免解碼模糊問題。模擬結果顯示在高次調變的系統中，前送策略的選擇，包括是否使用摺疊前送以及該選擇何種摺疊閾值等，必須根據通道狀態、端點站的調變型態及訊號強度來進行調整。



Study on Forwarding Strategies for Wireless Bidirectional Relay Transmission

Student: Shih-Jung Lu

Advisor: Dr. David W. Lin

Department of Electronics Engineering

Institute of Electronics

National Chiao Tung University

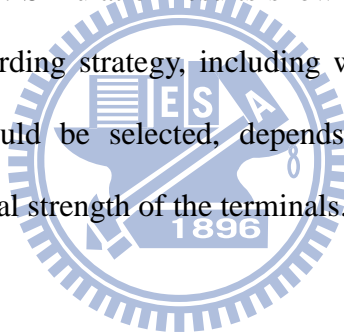


This thesis introduces the forwarding strategies for wireless bidirectional relay transmission. In bidirectional relay transmission, a relay receives simultaneously arrived signals from two terminals and then forwards the mixture of signals to the terminals. With the help of self data, each terminal can extract desired data from the received mixing signal.

In this thesis, we first give a brief overview on relay transmission models and the two basic forwarding strategies: amplify-and-forward (AF) and decode-and-forward (DF). Then we focus on an AF-based forwarding strategy, which we termed *fold-and-forward* (FF). We discuss the relay operation and the corresponding detection rule at the terminals in a FF system with BPSK modulation. We also give error analysis in a two-dimensional signal plane, which simplifies the symbol error

probability expression of FF system from a double integration into a sum of single integrations. Simulation results show that in an uncoded system, FF provides 1-1.5 dB gain over AF in high signal-to-noise ratio (SNR) region when the channels are symmetric. “The channels are symmetric” means that the two terminal-to-relay links have the same channel gain. The performance gain of FF system degrades when the channels become asymmetric.

Then we consider FF system with higher order modulation. In higher order modulation system, the design of FF operation must avoid a decoding ambiguity problem, which means that the terminal cannot distinguish data from the other terminal with the help of self data. We address the use of a proper folding threshold to avoid the ambiguity problem. Simulation results show that in high order modulation system, the choice of forwarding strategy, including whether to use FF or not and what folding threshold should be selected, depends on the channel conditions, modulation type and the signal strength of the terminals.



誌謝

本篇論文的完成，首先必須由衷地感謝我的指導教授林大衛博士。自大學時代的電子專題開始，老師便以其一貫親切樂觀的態度帶領我享受研究的樂趣。在我研究陷入困頓時，花費許多心力與我一起討論，共同解決遭遇的困難。在我犯錯沮喪時，給予我關懷與鼓勵，讓我重新找回熱情。謝謝您，老師。

接著必須感謝吳俊榮學長，每星期與老師的共同討論後，總是熱心地給我相當實用的建議，並且不厭其煩地與我討論我所遇到的問題。謝謝你，俊榮學長。

再來必須感謝通訊電子與訊號處理實驗室的所有成員，包括各位老師、學長姐以及學弟妹，讓 CommLab 成為一個歡樂的大家庭，讓我能夠在一個輕鬆愉快的環境中進行研究。

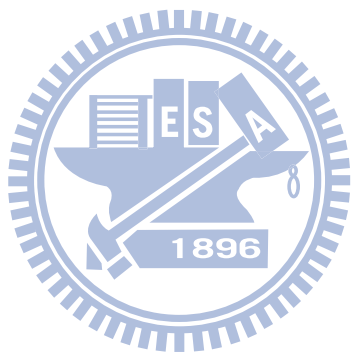
也要感謝陪伴我的同學及朋友們，你們豐富了我的人生，開拓了我的視野，讓我在感到苦悶時能轉換心情，體會生活其他美好有趣的一面。

最後，一定要感謝的，是我的家人們。因為有你們的支持與鼓勵，才能讓我勇敢而無所顧慮地在這條路上一直走下去。謝謝你們，親愛的阿嬤、爸媽、老哥、老弟。

在此，將這篇論文獻給所有幫助過我、伴我走過這段歲月的師長、同學、朋友以及家人。

盧世榮

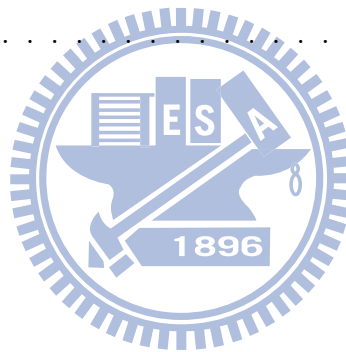
民國九十九年七月 於新竹



Contents

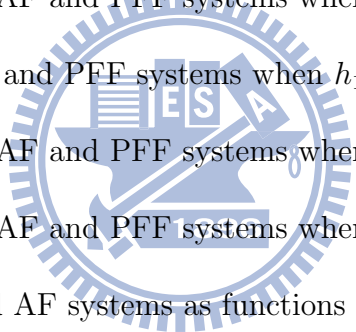
1	Introduction	1
1.1	Scope of the Work	1
1.2	Organization of This Thesis	3
2	Overview of Relay Transmission Model and Forwarding Strategies	4
2.1	Relay Transmission Model	4
2.2	Conventional Relay Forwarding Strategies	6
2.2.1	Amplify-and-Forward	7
2.2.2	Decode-and-Forward	10
3	Fold-and-Forward Bidirectional Relay System under BPSK Modulation	16
3.1	System Model	16
3.2	Power Scaling	18
3.3	Detection Rule	20
3.4	Error Analysis	25
3.5	Simulation Results	29

4	Fold-and-Forward Bidirectional Relay System with Higher-Order Modulations	44
4.1	System Model	45
4.2	Power Scaling	47
4.3	Detection Rule	47
4.4	Error Analysis	51
4.5	Simulation Results	54
5	Conclusion and Future Work	66
5.1	Conclusion	66
5.2	Possible Future Work	67
	Bibliography	68

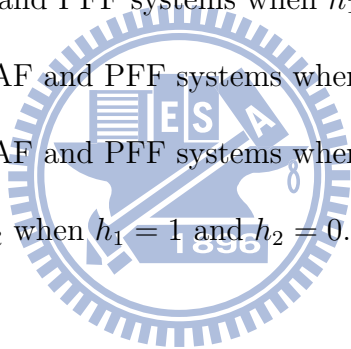


List of Figures

2.1	The three-node model in relay transmission.	6
2.2	Scheduling protocols of relay transmission.	7
2.3	Illustration of different forwarding points in the signal processing flow of a relay.	8
2.4	Signal flow of AF in four phase transmission.	11
2.5	Signal flow of AF in three phase transmission.	11
2.6	Signal flow of AF in two phase transmission.	12
2.7	Signal flow of DF in four phase transmission.	14
2.8	Signal flow of DF in three phase transmission.	14
2.9	Signal flow of DF in two phase transmission.	15
3.1	System model.	18
3.2	The signal folding operation.	20
3.3	Illustration of approximated Y_1 distribution.	24
3.4	A signal point S on two-dimensional plane with circularly symmetric complex AWGN. Sector AOC is the decision region.	27
3.5	The decision boundary of FF system for $T1$	29
3.6	Shaded area is the error region when $m = a + b$	30

3.7	Shaded area is the error region when $m = a - b$	30
3.8	Shaded area is the error region when $m = -a + b$	31
3.9	Shaded area is the error region when $m = -a - b$	31
3.10	The decision boundary of FF system for $T1$ when $w = -a$	32
3.11	Overall BER of FF, AF and PFF systems when $h_1 = 1$ and $h_2 = 1$	34
3.12	BER of $T1$ data of FF, AF and PFF systems when $h_1 = 1$ and $h_2 = 1$	35
3.13	BER of $T2$ data of FF, AF and PFF systems when $h_1 = 1$ and $h_2 = 1$	36
3.14	Overall BER of FF, AF and PFF systems when $h_1 = 1$ and $h_2 = 0.8$	37
3.15	BER of $T1$ data of FF, AF and PFF systems when $h_1 = 1$ and $h_2 = 0.8$	38
3.16	BER of $T2$ data of FF, AF and PFF systems when $h_1 = 1$ and $h_2 = 0.8$	39
3.17	Overall BER of FF, AF and PFF systems when $h_1 = 1$ and $h_2 = 0.5$	40
3.18	BER of $T1$ data of FF, AF and PFF systems when $h_1 = 1$ and $h_2 = 0.5$	41
3.19	BER of $T2$ data of FF, AF and PFF systems when $h_1 = 1$ and $h_2 = 0.5$	42
3.20	Overall BERs of FF and AF systems as functions of WSANR and h_2	43
		
4.1	Block diagram for OFDM system with FF.	45
4.2	System model.	46
4.3	Signal distribution seen at $T2$ when $w = -2a$ and $T2$ sends $+B$	49
4.4	Signal distribution seen at $T2$ when $w = -2a$ and $T2$ sends $-B$	49
4.5	Decision boundaries of the 4PAM+BPSK FF system for $T2$ when $w = 0$	51
4.6	Decision boundaries of the 4PAM+BPSK FF system for $T2$ when $w \neq 0$	52

4.7	Relay signal value sets of the 4PAM+BPSK FF system when $a = b$ in absence of AWGN.	53
4.8	Overall SER of FF, AF and PFF systems when $h_1 = 1$ and $h_2 = 1$	55
4.9	SER of T1 data of FF, AF and PFF systems when $h_1 = 1$ and $h_2 = 1$	56
4.10	SER of T2 data of FF, AF and PFF systems when $h_1 = 1$ and $h_2 = 1$	57
4.11	Overall SER of FF, AF and PFF systems when $h_1 = 1$ and $h_2 = 0.8$	58
4.12	SER of T1 data of FF, AF and PFF systems when $h_1 = 1$ and $h_2 = 0.8$	59
4.13	SER of T2 data of FF, AF and PFF systems when $h_1 = 1$ and $h_2 = 0.8$	60
4.14	Signal distribution of Y_R when $h_1 = 1$ and $h_2 = 0.8$	61
4.15	Overall SER of FF, AF and PFF systems when $h_1 = 1$ and $h_2 = 0.5$	62
4.16	SER of T1 data of FF, AF and PFF systems when $h_1 = 1$ and $h_2 = 0.5$	63
4.17	SER of T2 data of FF, AF and PFF systems when $h_1 = 1$ and $h_2 = 0.5$	64
4.18	Signal distribution of Y_R when $h_1 = 1$ and $h_2 = 0.5$	65





Chapter 1

Introduction

1.1 Scope of the Work

With the increasing need of high quality multimedia and communication services, high rate digital wireless transmission over large areas has been gaining more and more research interests. The next generation communication standards, such as IEEE 802.16m and 3GPP LTE-Advanced, have included many promising techniques to achieve the goal of high-rate, high-mobility, high-coverage and high-system-capacity transmission. Among these techniques, relaying has attracted a lot of attentions. The concept of relaying is to enhance the system performance and extend coverage areas by employing several simple and low-cost relay stations between source and destination terminals.

There are many interesting research issues related to the relay transmission. For example, the precoding [2], [21], the space time coding [16], [19] and the relay selection [11], [12] are just some of the topics. Channel estimation [8], [9] and synchronization [4], [15] are some other issues. Our work focus on the forwarding operation in the relay system. More specifically, the relay system we considered in this thesis is bidirectional relay, also known as two-way relay network (TWRN), in which it takes only two time slots to exchange information between two terminals. The fundamental of bidirectional relay can be traced back

to Claude E. Shannon in 1961 [18], where the achievable rate of two-way communication channel is analyzed. However, it is not until recent that the bidirectional relay transmission begin to gain research interests [1], [3], [10], [13], [17], [20], [23]. A bidirectional relay system is regarded spectral-efficient comparing to the traditional relay, where the exchange of information between two terminals takes four time slots. The mechanism of bidirectional relay is conceptually easy but hard to analyze. However, through the step-by-step discussion on a novel forwarding operation in the bidirectional relay systems, we hope to establish some basis for future studies on forwarding strategy design while providing simpler analytical results on error performance.

In this thesis, our work can be summarized as following:

- Study relay transmission model.
- Study conventional forwarding strategies in relay systems.
- Study a novel forwarding strategy, termed as fold-and-forward (FF), for bidirectional relay systems.
 - Study the relay forwarding operation in FF systems.
 - Analyze the error performance of FF systems.
 - Discuss on the selection of forwarding method at the relay station.

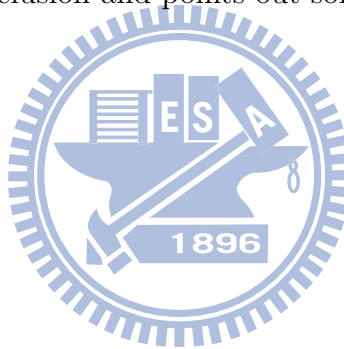
Main contributions of this thesis are as follows:

1. Introduce FF for bidirectional relay.
2. Include a parameter, the folding threshold, for FF design.
3. Develop an error analysis scheme for relay systems.
4. Provide guidelines for designing relay forwarding strategies.

1.2 Organization of This Thesis

This thesis is organized as follows.

- Chapter 2 introduces relay transmission model and conventional forwarding strategies in relay systems.
- Chapter 3 discusses a novel forwarding strategy in bidirectional relay systems with binary-phase shift keying (BPSK).
- Chapter 4 extends discussion on forwarding strategy to systems employing higher order modulation.
- Chapter 5 contains the conclusion and points out some future work.



Chapter 2

Overview of Relay Transmission Model and Forwarding Strategies

In this chapter, we first introduce three relay transmission models. Then we give an overview of the typical forwarding strategies used in relay systems. The contents of this chapter are mostly arranged from the contents of [6], [7], [14], [20], [22] and [23].

2.1 Relay Transmission Model

A common relay system model is the “three-node model” shown in Fig. 2.1. The system is composed of two terminal nodes and one relay node, where each node may have a single or multiple antennas. The terminals exchange their messages through the help of the relay. There are two possible scenarios:

1. There *does not exist* a direct link between the two terminals. The relay is necessary for communication between the terminals.
2. There *exists* a direct link between the two terminals. The relay is used to enhance the system capacity or provide diversity.

An example of the first scenario is that when the relays are used to provide coverage extension. On the other hand, in the second scenario, relays are used to improve the transmission quality. In general, the second scenario provides more flexibility in signal processing techniques. For simplicity, in this thesis we only consider the first scenario with each node having only one single antenna.

Under the first scenario, there are three different scheduling protocols:

1. *Four phase* scheduling is shown in Fig. 2.2(a). It requires four time slots to complete one exchange of messages.
2. *Thress phase* scheduling is shown in Fig. 2.2(b). It needs three time slots to complete one exchange of messages.
3. *Two phase* scheduling is shown in Fig. 2.2(c). It takes two time slots to complete one exchange of messages.

Four phase scheduling is the traditional relaying protocol. In such a protocol, terminal 1 transmits its data to the relay in the first time slot. Then the relay forwards the information to terminal 2 in the second time slot. In the third time slot, terminal 2 transmits its data to the relay and the relay forwards the information in the last time slot to complete one exchange of messages. Many existing signal processing techniques can be applied directly to four phase protocol, since the data of the two terminals are transmitted separately. However, the drawback of is the latency and bandwidth inefficiency; in the conventional relayless transmission, only two time slots are needed for a complete message exchange. To reduce latency and improve bandwidth efficiency, some studies [7], [13] outline the use of the three phase protocol, in which the terminals separately transmit their data to the relay in two time slots and the relay may perform binary XOR on the decoded data. Then the relay broadcasts the resulting signal in the third time slot. The terminals, after receiving the

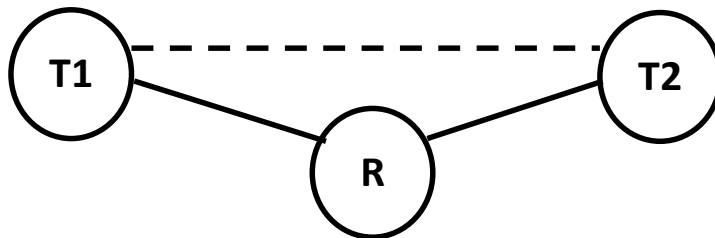


Figure 2.1: The three-node model in relay transmission.

signal, may perform binary XOR of the decoded data with its own transmitted data to extract the desired data from the other terminal. This protocol reduces the required time slots for message change from four to three. Some recent studies [17], [23] exploit the superpositioning nature of electronic magnetic waves and propose the use of the two phase protocol. The two terminals simultaneously transmit their own data to the relay in the first time slot. Assuming that the terminals have perfect synchronization and their data arrive at the relay at the same time, the relay receives a signal consisting of the sum of the two data plus noise. Then the relay forwards the signal to both terminals in the second time slot. The terminals subtract the self-data component from the received signal and decode the desired data. This protocol further compresses the required time slots to two. Our work mainly considers the forwarding operation under the two phase protocol.

2.2 Conventional Relay Forwarding Strategies

Forwarding strategy is one of the most important features that determines the system performance and the relay complexity in a relay system. As shown in Fig. 2.3, there are several forwarding points in the signal processing flow at the relay. When the forwarding is performed earlier in the flow, the relay has less processing complexity and incurs less delay. When the forwarding is performed later in the flow, the relay mitigates the noise effect and

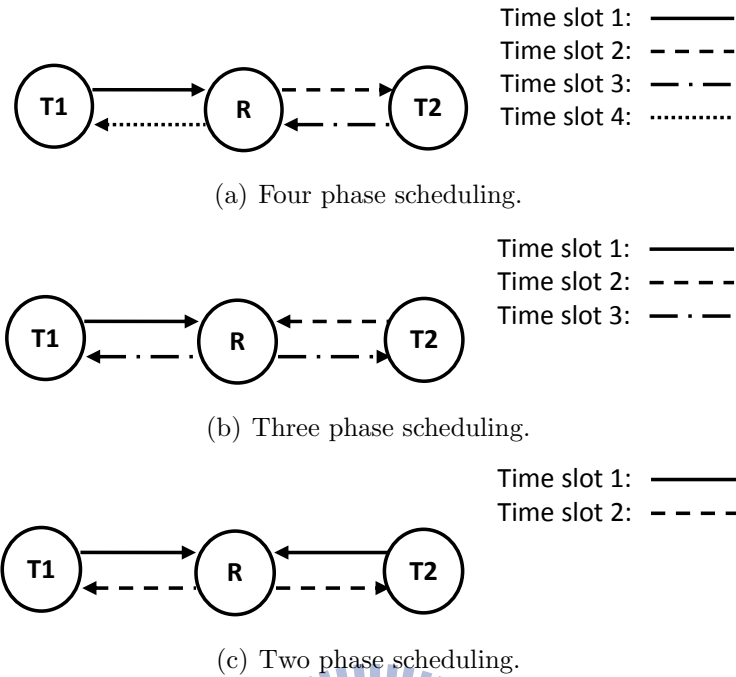


Figure 2.2: Scheduling protocols of relay transmission.

provides better system performance. In what follows, we give an overview on two basic classes of forwarding strategies: amplify-and-forward (AF) and decode-and-forward (DF). An AF relay does not decode the received signal but forwards the amplified signal directly. A DF relay decodes the received signal, re-encodes the result and then forwards the signal to the destination. In general, when signal-to-noise ratio (SNR) is high, a DF relay has better error performance at the cost of higher complexity and decoding latency. For more details concerning AF and DF, we refer readers to [14] and the references therein.

2.2.1 Amplify-and-Forward

An amplify-and-forward relay, as it is named, simply amplifies its received signal and then forwards the result to the destination. We introduce the AF system for the three scheduling protocols in the following.

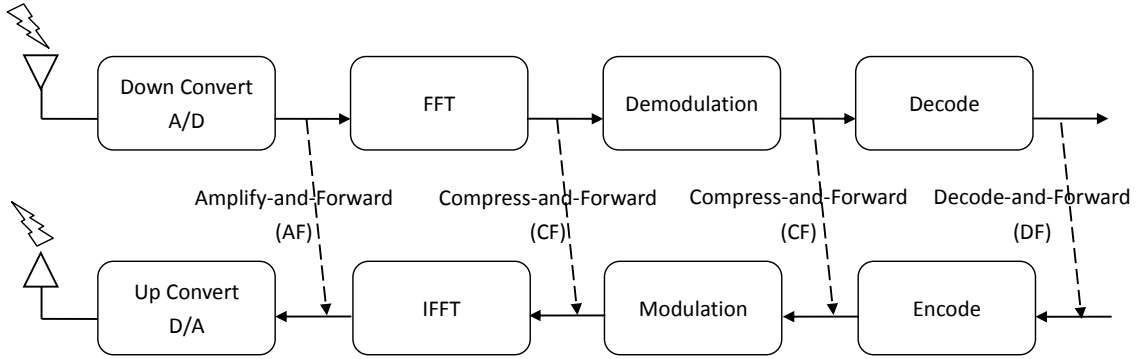


Figure 2.3: Illustration of different forwarding points in the signal processing flow of a relay.

In the four phase protocol, the signal transmission flow is shown in Fig. 2.4. At the end of time slot 1, the relay receives

$$Y_{R,1} = h_1 \sqrt{P_{S,1}} X_1 + N_1 \quad (2.1)$$

with $\sqrt{P_{S,1}}$ being the transmission power of $T1$, h_1 the channel gain between $T1$ and the relay, and N_1 the additive noise at the relay in time slot 1 which has zero mean and variance $\sigma_{N_1}^2$. In time slot 2, the relay transmits signal

$$X_{R,1} = \beta_1 Y_{R,1} \quad (2.2)$$

to $T2$, with β_1 being the power scaling factor that is inversely proportional to the received power and given by

$$\beta_1 = \sqrt{\frac{P_R}{P_{S,1}|h_1|^2 + \sigma_{N_1}^2}}. \quad (2.3)$$

The received signal at $T2$ is therefore

$$Y_2 = h_2 \sqrt{\frac{P_R}{P_{S,1}|h_1|^2 + \sigma_{N_1}^2}} Y_{R,1} + Z_2. \quad (2.4)$$

For time slots 3 and 4, the transmission is in the opposite direction and the received signal at $T1$ is

$$Y_1 = h_4 \sqrt{\frac{P_R}{P_{S,2}|h_3|^2 + \sigma_{N_2}^2}} Y_{R,2} + Z_1 \quad (2.5)$$

with

$$Y_{R,2} = h_3\sqrt{P_{S,2}}X_2 + N_2.$$

The decoding of the desired data under the four phase protocol is based on Y_1 and Y_2 .

The signal transmission flow in the three phase protocol is shown in Fig. 2.5. In time slots 1 and 2, the relay receives, respectively,

$$Y_{R,1} = h_1\sqrt{P_{S,1}}X_1 + N_1, \quad Y_{R,2} = h_2\sqrt{P_{S,2}}X_2 + N_2. \quad (2.6)$$

In time slot 3, the relay linearly combines $Y_{R,1}$ and $Y_{R,2}$ with weights k_1 and k_2 , and then scales the result with β . The broadcasted signal is

$$X_R = \beta(k_1Y_{R,1} + k_2Y_{R,2}) \quad (2.7)$$

where

$$\beta = \sqrt{\frac{P_R}{P_{S,1}|k_1|^2|h_1|^2 + P_{S,2}|k_2|^2|h_2|^2 + |k_1|^2\sigma_{N_1}^2 + |k_2|^2\sigma_{N_2}^2}}.$$

The received signals at $T1$ and $T2$ are

$$\begin{aligned} Y_1 &= h_{B1}\beta(k_1h_1\sqrt{P_{S,1}}X_1 + k_2h_2\sqrt{P_{S,2}}X_2) + h_{B1}\beta(k_1N_1 + k_2N_2) + Z_1, \\ Y_2 &= h_{B2}\beta(k_1h_1\sqrt{P_{S,1}}X_1 + k_2h_2\sqrt{P_{S,2}}X_2) + h_{B2}\beta(k_1N_1 + k_2N_2) + Z_2, \end{aligned} \quad (2.8)$$

respectively. Assume that the terminals have perfect channel state information (CSI), the terminals subtract the self data component from the received signals and obtain

$$\begin{aligned} \tilde{Y}_1 &= h_{B1}\beta(k_2h_2\sqrt{P_{S,2}}X_2) + h_{B1}\beta(k_1N_1 + k_2N_2) + Z_1, \\ \tilde{Y}_2 &= h_{B2}\beta(k_1h_1\sqrt{P_{S,1}}X_1) + h_{B2}\beta(k_1N_1 + k_2N_2) + Z_2. \end{aligned} \quad (2.9)$$

Therefore, the decoding of the desired data in the three phase protocol is based on \tilde{Y}_1 and \tilde{Y}_2 .

In the two phase protocol, the AF signal transmission is shown in Fig. 2.6. In time slot 1, the relay receives signal

$$Y_R = h_1\sqrt{P_{S,1}}X_1 + h_2\sqrt{P_{S,2}}X_2 + N. \quad (2.10)$$

And in time slot 2, the relay scales the signal and broadcasts

$$X_R = \beta Y_R \quad (2.11)$$

with

$$\beta = \sqrt{\frac{P_R}{P_{S,1}|h_1|^2 + P_{S,2}|h_2|^2 + \sigma_N^2}}.$$

The terminals receive

$$\begin{aligned} Y_1 &= h_{B1}\beta(h_1\sqrt{P_{S,1}}X_1 + h_2\sqrt{P_{S,2}}X_2 + N) + Z_1, \\ Y_2 &= h_{B2}\beta(h_1\sqrt{P_{S,1}}X_1 + h_2\sqrt{P_{S,2}}X_2 + N) + Z_2, \end{aligned} \quad (2.12)$$

respectively. After subtracting the self data, the decoding of desired data is based on

$$\begin{aligned} \tilde{Y}_1 &= h_{B1}\beta(h_2\sqrt{P_{S,2}}X_2) + h_{B1}\beta N + Z_1, \\ \tilde{Y}_2 &= h_{B2}\beta(h_1\sqrt{P_{S,1}}X_1) + h_{B2}\beta N + Z_2. \end{aligned} \quad (2.13)$$

2.2.2 Decode-and-Forward

A decode-and-forward relay decodes the received signal, re-encodes it, and then transmits the result to the destination. Since the relay performs decoding before transmission, the forwarded signal is clean without additive noise from the relay reception. However, the decoding may be incorrect, which may cause error propagation and diminish the performance of the system. In the following, we introduce DF system for the three scheduling protocols.

The DF signal transmission in the four phase protocol is shown in Fig. 2.7. In time slot 1, the relay receives

$$Y_{R,1} = h_1\sqrt{P_{S,1}}X_1 + N_1. \quad (2.14)$$

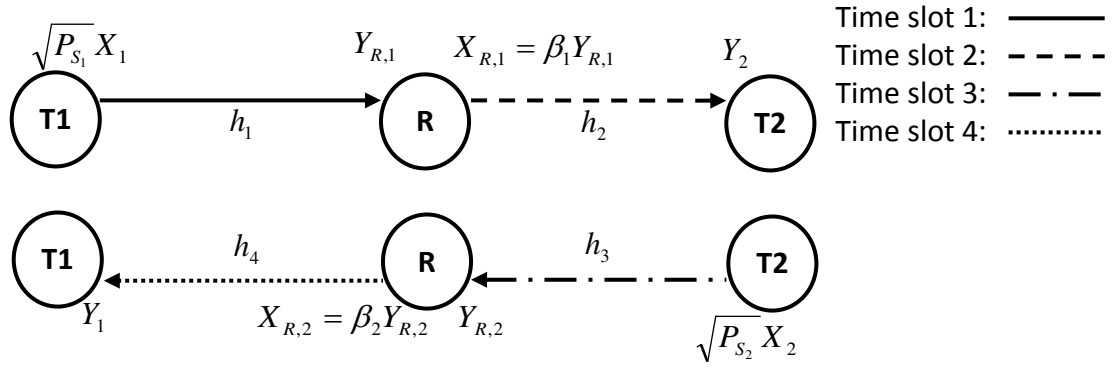


Figure 2.4: Signal flow of AF in four phase transmission.

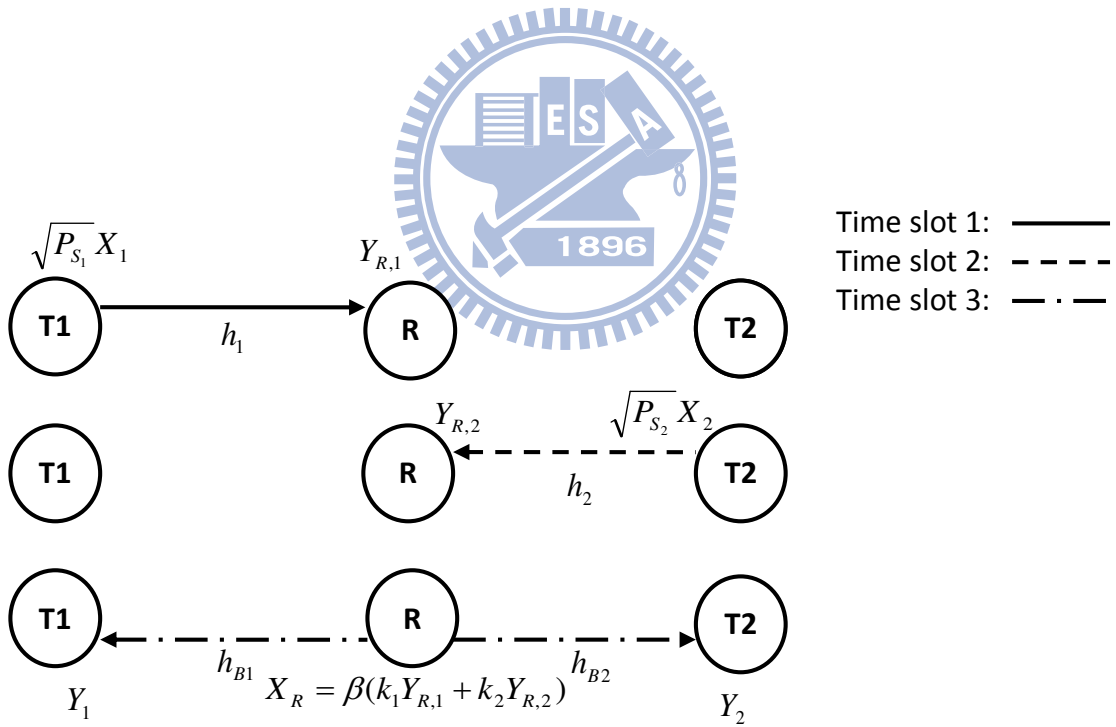


Figure 2.5: Signal flow of AF in three phase transmission.

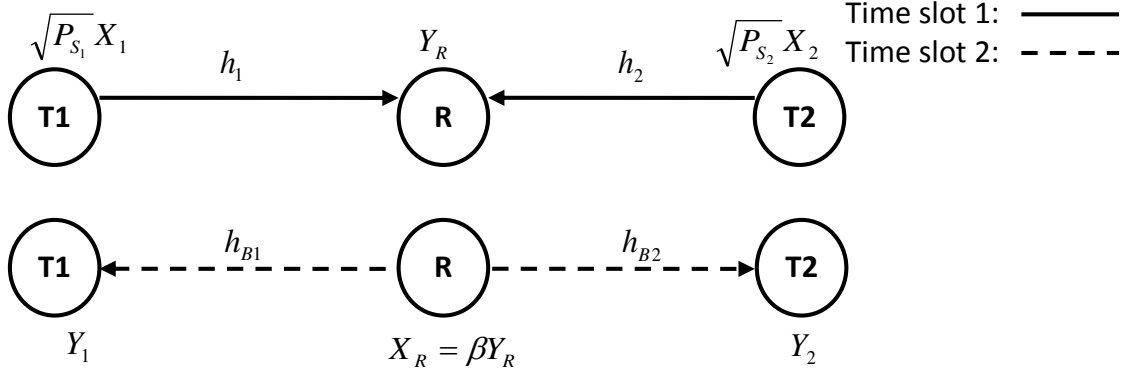


Figure 2.6: Signal flow of AF in two phase transmission.

Based on this received signal, relay decodes the $T1$ data as \hat{X}_1 and transmits in time slot 2 the signal

$$X_{R,1} = \sqrt{P_R} \hat{X}_1. \quad (2.15)$$

Terminal $T2$ decodes the $T1$ data based on the received signal

$$Y_2 = h_2 \sqrt{P_R} \hat{X}_1 + Z_2. \quad (2.16)$$

Following a similar procedure in time slots 3 and 4, terminal $T1$ decodes the $T2$ data based on its received signal

$$Y_1 = h_1 \sqrt{P_R} \hat{X}_2 + Z_1 \quad (2.17)$$

where \hat{X}_2 is relay's decoding result of the $T2$ data.

The DF signal transmission in the three phase protocol is shown in Fig. 2.8. In time slots 1 and 2, the relay decodes the $T1$ and $T2$ data as \hat{X}_1 and \hat{X}_2 based on the received signal

$$Y_{R,1} = h_1 \sqrt{P_{S,1}} X_1 + N_1, \quad Y_{R,2} = h_2 \sqrt{P_{S,2}} X_2 + N_2, \quad (2.18)$$

respectively. In time slot 3, the relay performs XOR on the decoded binary data \hat{X}_1 and \hat{X}_2 and broadcasts to $T1$ and $T2$ the signal

$$X_R = \sqrt{P_R} (\hat{X}_1 \oplus \hat{X}_2). \quad (2.19)$$

The received signal at terminals $T1$ and $T2$ are

$$Y_1 = h_{B1}\sqrt{P_R}(\hat{X}_1 \oplus \hat{X}_2) + Z_1, \quad Y_2 = h_{B2}\sqrt{P_R}(\hat{X}_1 \oplus \hat{X}_2) + Z_2, \quad (2.20)$$

respectively. Each terminal performs decoding to obtain its estimation of $\hat{X}_1 \oplus \hat{X}_2$ and then performs XOR on the result with self data to recover the data from the other terminal.

The DF signal transmission in the two phase protocol is shown in Fig. 2.9. In time slot 1, the relay receives signal

$$Y_R = h_1\sqrt{P_{S,1}}X_1 + h_2\sqrt{P_{S,2}}X_2 + N. \quad (2.21)$$

The relay performs hard decision on Y_R and maps each decision region to a fixed value and broadcasts in time slot 2 the signal

$$X_R = \beta C(Y_R), \quad (2.22)$$

where the function $C(\cdot)$ makes hard decision on Y_R and maps the result to a value in a fixed codeword set S and scaling factor β is given by

$$\beta = \sqrt{\frac{P_R}{E_s}} \quad (2.23)$$

with E_s representing the average power of signals in the codeword set. Terminals $T1$ and $T2$ receive signals

$$\begin{aligned} Y_1 &= h_{B1}\sqrt{\frac{P_R}{E_s}}C(Y_R) + Z_1, \\ Y_2 &= h_{B2}\sqrt{\frac{P_R}{E_s}}C(Y_R) + Z_2, \end{aligned} \quad (2.24)$$

respectively. With the help of self data, each terminal then finds the most possible codeword in S and recovers the desired data from the other terminal.

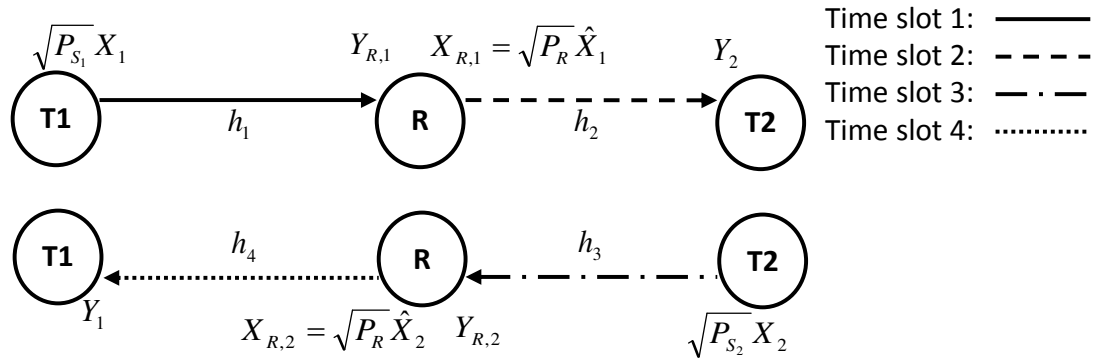


Figure 2.7: Signal flow of DF in four phase transmission.

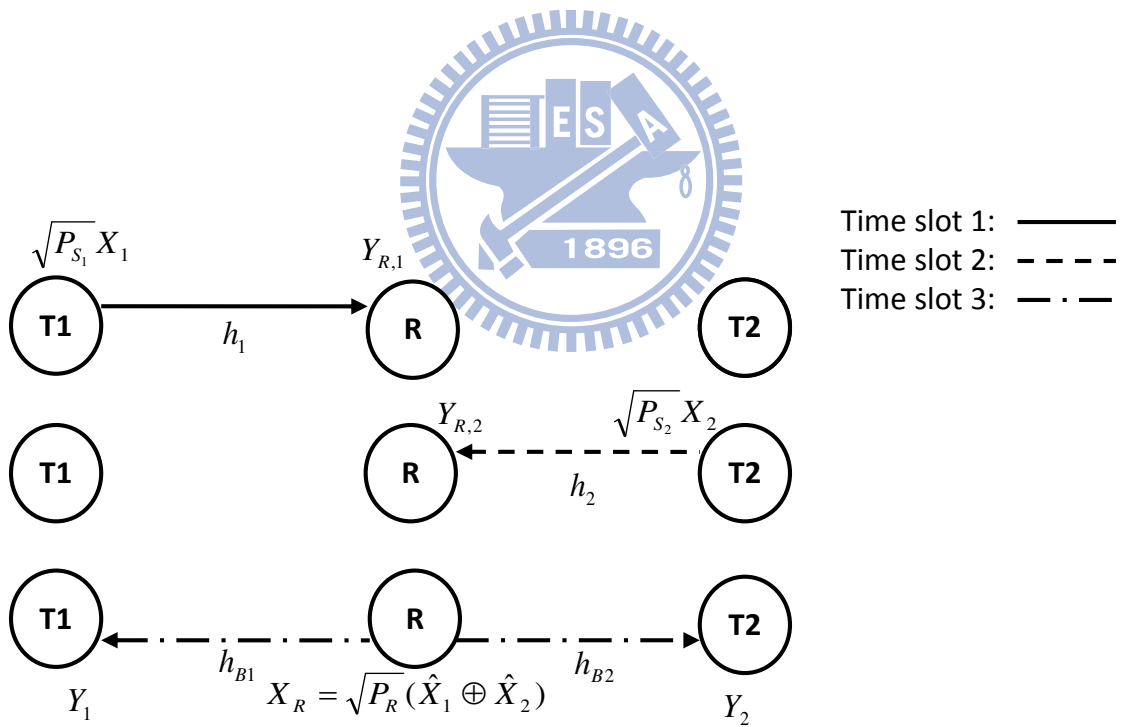


Figure 2.8: Signal flow of DF in three phase transmission.

Chapter 3

Fold-and-Forward Bidirectional Relay System under BPSK Modulation

In our work, we consider a bidirectional relay system that employs an AF-based forwarding strategy. The relay takes absolute value on its received signal and, after proper power scaling, it broadcasts the resulting signal to the destination terminals. We call the above relay operation as “fold-and-forward (FF),” since the operation forwards a signal whose distribution is a folded-version of the signal forwarded in a conventional AF system. In this chapter, we discuss how to perform FF and analyze the corresponding symbol error rate (SER). We assume that the system is uncoded and both terminals transmit BPSK signals; we leave the discussion on higher order modulation to the next chapter.

3.1 System Model

The system model is illustrated in Fig. 3.1, where X_i is the datum from terminal T_i , $i = 1, 2$, and A and B are the transmitted signal amplitudes of T_1 and T_2 data. Y_R , X_R , and Y_i are the received signal at the relay, the transmitted signal at the relay, and the received signal at the terminal i , respectively. The communication involves two time phases. Phase 1 is called the multiple access (MAC) phase, when both terminals simultaneously transmit

a block of data symbols to the relay and generates at each symbol time a received signal given by $Y_R = h_1AX_1 + h_2BX_2 + N$. The quantity h_i is the channel gain from T_i to the relay and we assume that $h_1 \geq h_2 \geq 0$ without loss of generality. We also assume that the channels are known to all the terminals and the relay, and that the terminals compensate the phase rotation caused by the channels. The quantity N is the additive white Gaussian noise (AWGN) at the relay with zero mean and variance σ_N^2 . For notational simplicity, we define $a = Ah_1$, $b = Bh_2$ and $M = aX_1 + bX_2$ and assume that $a \geq b$.

In phase 2, the broadcast (BC) phase, the relay transmits an operated signal $X_R = f(Y_R)$ to both terminals T_1 and T_2 . The relay operation function $f(\cdot)$ takes the absolute value of the received signal if it is under certain threshold $w \leq 0$ and then subtracts a positive constant C from the resulting signal to remove the DC bias from the signal. The function $f(\cdot)$ can therefore be written as

$$f(u) = \begin{cases} \beta(|u| - C), & \text{if } u < w, \\ \beta(u - C), & \text{otherwise.} \end{cases} \quad (3.1)$$

where β is the power scaling factor to satisfy the power constraint at the relay. We will discuss this power scaling factor later on in section 3.2.

During the BC phase, terminal i receives the signal $Y_i = h_iX_R + Z_i$, $i = 1, 2$, where Z_i represents the zero mean AWGN with variance $\sigma_{Z_i}^2$ at terminal i . Here, we assume that channel reciprocity holds and that the channel is invariant during the 2 phases. Since each terminal knows what itself sends to the relay in the MAC phase, it can use its own data as *a priori* information to detect the other terminal's data embedded in the received Y_i . More detailed discussion on the detection rule will be given in section 3.3.

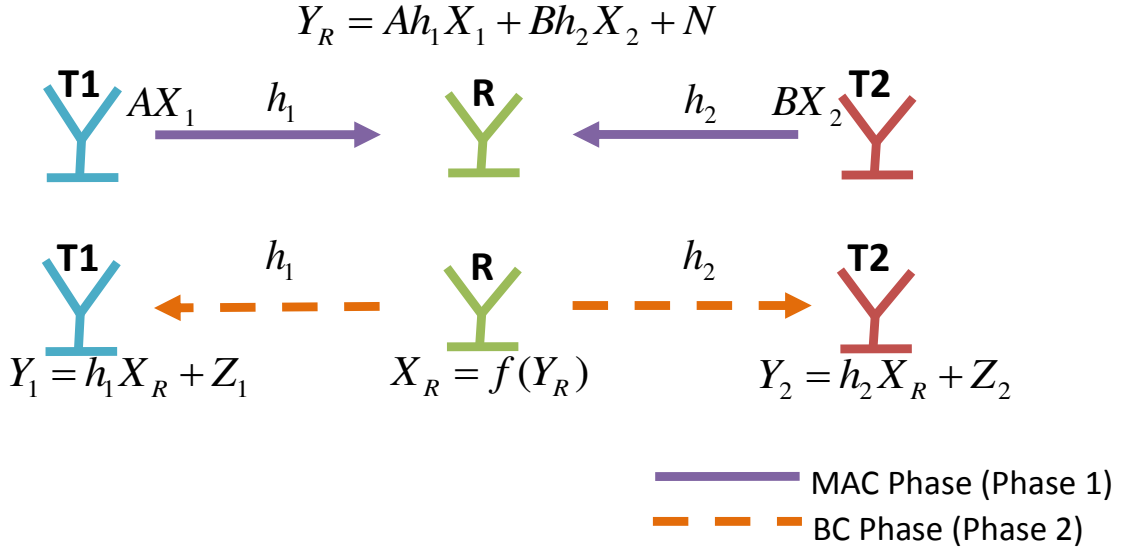


Figure 3.1: System model.

3.2 Power Scaling

To maintain a certain fixed average transmission power, the relay must multiply a power scaling factor β to the signal before forwarding it to the destination terminals. In an AF system, this scaling factor can be easily obtained as the power constraint P_R divided by the average power of Y_R . However, in an FF system, the relay received signal Y_R is folded and DC-removed. The average power of this operated signal \tilde{Y}_R has to be recalculated. For this, since we have

$$\tilde{Y}_R = \begin{cases} |Y_R| - C, & \text{if } Y_R < w, \\ Y_R - C, & \text{otherwise,} \end{cases} \quad (3.2)$$

the average power of \tilde{Y}_R is:

$$\begin{aligned}
E[|\tilde{Y}_R|^2] &= \int_{-\infty}^{\infty} p_{\tilde{Y}_R} |\tilde{Y}_R|^2 d\tilde{Y}_R \\
&= \int_{-\infty}^w p_{Y_R} (|Y_R|^2 + C^2 - 2|Y_R|C) dY_R + \int_w^{\infty} p_{Y_R} (|Y_R|^2 + C^2 - 2Y_R C) dY_R \\
&= \int_{-\infty}^{\infty} p_{Y_R} |Y_R|^2 dY_R + \int_{-\infty}^{\infty} p_{Y_R} C^2 dY_R - 2C \left(\int_{-\infty}^w p_{Y_R} |Y_R| dY_R + \int_w^{\infty} p_{Y_R} Y_R dY_R \right) \\
&= \int_{-\infty}^{\infty} p_{Y_R} |Y_R|^2 dY_R + C^2 - 2CJ, \tag{3.3}
\end{aligned}$$

where p_{Y_R} is the probability distribution of signal Y_R .

The first term in the last right-hand side of (3.3) is the average power of Y_R , which is equal to $a^2 + b^2 + \sigma_n^2$ in the BPSK case. The second and the last terms together represent the power reduced by the folding operation. We have defined $J \triangleq \int_{-\infty}^w p_{Y_R} |Y_R| dY_R + \int_w^{\infty} p_{Y_R} Y_R dY_R$ and the work now is to calculate this J value. Since both terminals transmit BPSK signals, the relay receives a signal with value $M = aX_1 + bX_2$ in the set $S = \{a + b, a - b, -a + b, -a - b\}$ plus relay noise N . Assume that the value of $M = m$ is known, the distribution of the received signal r at the relay is $N(m, \sigma_N^2)$. As shown in Fig. 3.2, the signal value below $w \leq 0$ is folded (taken absolute value), i.e.,

$$\tilde{r} = \begin{cases} -r, & \text{if } r < w, \\ r, & \text{otherwise.} \end{cases} \tag{3.4}$$

Therefore, we have

$$\begin{aligned}
\int p_{\tilde{r}} \tilde{r} d\tilde{r} &= \int_{-\infty}^w p_r(-r) dr + \int_w^{\infty} p_r r dr \\
&= \left[\frac{\sigma_N}{\sqrt{2\pi}} \exp\left(-\frac{(m-w)^2}{2\sigma_N^2}\right) - mQ\left(\frac{m-w}{\sigma_N}\right) \right] \\
&\quad + \left[\frac{\sigma_N}{\sqrt{2\pi}} \exp\left(\frac{(m-w)^2}{2\sigma_N^2}\right) + mQ\left(-\frac{m-w}{\sigma_N}\right) \right] \\
&= \frac{\sigma_N}{\sqrt{2\pi}} \left[\exp\left(-\frac{(m-w)^2}{2\sigma_N^2}\right) + \exp\left(\frac{(m-w)^2}{2\sigma_N^2}\right) \right] \\
&\quad + m \left[Q\left(-\frac{m-w}{\sigma_N}\right) - Q\left(\frac{m-w}{\sigma_N}\right) \right] \\
&\triangleq G(m, w). \tag{3.5}
\end{aligned}$$

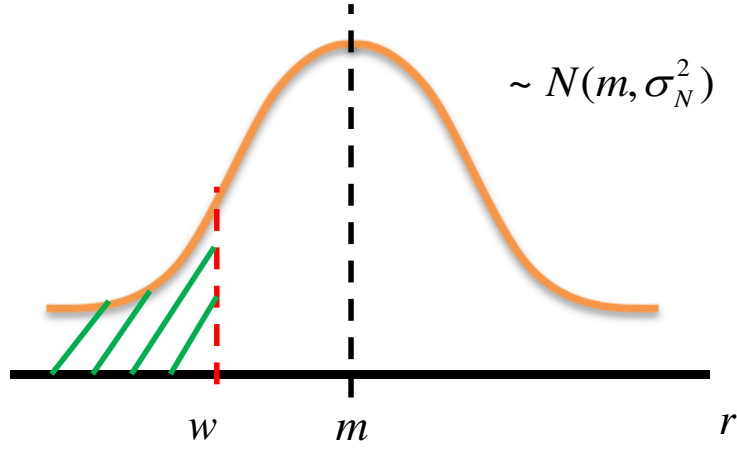


Figure 3.2: The signal folding operation.

Now, we may get the value of J as

$$\begin{aligned}
 J &= \sum_{m \in \mathcal{S}} p(m)G(m, w) \\
 &= \frac{1}{4}[G(a + b, w) + G(a - b, w) + G(-a + b, w) + G(-a - b, w)].
 \end{aligned} \tag{3.6}$$

The power scaling factor β for FF system is therefore given by

$$\begin{aligned}
 \beta &= \sqrt{\frac{P_R}{E[|\tilde{Y}_R|^2]}} \\
 &= \sqrt{\frac{P_R}{a^2 + b^2 + \sigma_N^2 + C^2 - 2CJ}}.
 \end{aligned} \tag{3.7}$$

One thing to note here is that the value of β depends on the values of w , C and σ_N^2 .

3.3 Detection Rule

One of the most important features of network coding is the utilization of self-data as *a priori* information to detect the desired data from the received mixture of signals. In an

FF system, even though the forwarded signal is distorted, the destination terminal can still recover the desired signal. However, the data detection at the terminals closely depends on the forwarding operation at the relay. More specifically, it depends on the choice of the folding threshold w . For the following discussion, we assume that $w = 0$, which is a reasonable choice in the BPSK + BPSK case. The detection rule for other choices of w can be derived in a similar way. First, consider the received-signal distribution at the destination terminals. At terminal $T1$, it receives

$$\begin{aligned}
Y_1 &= h_1 f(Y_R) + Z_1 \\
&= \begin{cases} h_1 \beta (-Y_R - C) + Z_1, & \text{if } Y_R < w, \\ h_1 \beta (Y_R - C) + Z_1, & \text{otherwise,} \end{cases} \\
&= \begin{cases} h_1 \beta (-(M + N) - C) + Z_1, & \text{if } (M + N) < w, \\ h_1 \beta ((M + N) - C) + Z_1, & \text{otherwise.} \end{cases} \tag{3.8}
\end{aligned}$$

Recall that $M = aX_1 + bX_2$. Consider the distribution of Y_R and Z_1 , assuming that $M = m$ is known. The conditional probability density function (conditional PDF) of Y_1 can be derived as

$$\begin{aligned}
f_{Y_1|M}(y_1|M = m) &= \frac{1}{\sqrt{2\pi}\sqrt{h_1^2\beta^2\sigma_N^2 + \sigma_Z^2}} \left[\exp\left(-\frac{(h_1\beta m - (y_1 + C))^2}{2(\sigma_Z^2 + h_1^2\beta^2\sigma_N^2)}\right) Q\left(\frac{w - \frac{\sigma_Z^2 h_1\beta m + h_1^2\beta^2\sigma_N^2(y_1 + C)}{\sigma_Z^2 + h_1^2\beta^2\sigma_N^2}}{\sqrt{\frac{h_1^2\beta^2\sigma_Z^2\sigma_N^2}{\sigma_Z^2 + h_1^2\beta^2\sigma_N^2}}}\right) \right. \\
&\quad \left. + \exp\left(-\frac{(h_1\beta m + (y_1 + C))^2}{2(\sigma_Z^2 + h_1^2\beta^2\sigma_N^2)}\right) Q\left(\frac{-w + \frac{\sigma_Z^2 h_1\beta m - h_1^2\beta^2\sigma_N^2(y_1 + C)}{\sigma_Z^2 + h_1^2\beta^2\sigma_N^2}}{\sqrt{\frac{h_1^2\beta^2\sigma_Z^2\sigma_N^2}{\sigma_Z^2 + h_1^2\beta^2\sigma_N^2}}}\right) \right]. \tag{3.9}
\end{aligned}$$

With (3.9), the receiver at $T1$ may apply the *maximum likelihood* (ML) principle to detect $T2$ data. That is:

- If $T1$ sends $+A$ in the MAC phase, the detection rule is

$$\hat{X}_2 = \begin{cases} +1, & \text{if } f_{Y_1|M}(y_1|a + b) \geq f_{Y_1|M}(y_1|a - b), \\ -1, & \text{if } f_{Y_1|M}(y_1|a + b) < f_{Y_1|M}(y_1|a - b). \end{cases} \tag{3.10}$$

- If $T1$ sends $-A$ in the MAC phase, the detection rule is

$$\hat{X}_2 = \begin{cases} +1, & \text{if } f_{Y_1|M}(y_1|-a + b) \geq f_{Y_1|M}(y_1|-a - b), \\ -1, & \text{if } f_{Y_1|M}(y_1|-a + b) < f_{Y_1|M}(y_1|-a - b). \end{cases} \tag{3.11}$$

Similarly, the conditional PDF of Y_2 can be derived as

$$f_{Y_2|M}(y_2|M = m) = \frac{1}{\sqrt{2\pi}\sqrt{h_2^2\beta^2\sigma_N^2 + \sigma_Z^2}} \left[\exp\left(-\frac{(h_2\beta m - (y_2 + C))^2}{2(\sigma_Z^2 + h_2^2\beta^2\sigma_N^2)}\right) Q\left(\frac{w - \frac{\sigma_Z^2 h_2\beta m + h_2^2\beta^2\sigma_N^2(y_2 + C)}{\sigma_Z^2 + h_2^2\beta^2\sigma_N^2}}{\sqrt{\frac{h_2^2\beta^2\sigma_Z^2\sigma_N^2}{\sigma_Z^2 + h_2^2\beta^2\sigma_N^2}}}\right) \right. \\ \left. + \exp\left(-\frac{(h_2\beta m + (y_2 + C))^2}{2(\sigma_Z^2 + h_2^2\beta^2\sigma_N^2)}\right) Q\left(\frac{-w + \frac{\sigma_Z^2 h_2\beta m - h_2^2\beta^2\sigma_N^2(y_2 + C)}{\sigma_Z^2 + h_2^2\beta^2\sigma_N^2}}{\sqrt{\frac{h_2^2\beta^2\sigma_Z^2\sigma_N^2}{\sigma_Z^2 + h_2^2\beta^2\sigma_N^2}}}\right) \right]. \quad (3.12)$$

And the corresponding ML detection rule is:

- If T_2 sends $+B$ in the MAC phase, the detection rule is

$$\hat{X}_1 = \begin{cases} +1, & \text{if } f_{Y_2|M}(y_2|a+b) \geq f_{Y_2|M}(y_2|-a+b), \\ -1, & \text{if } f_{Y_2|M}(y_2|a+b) < f_{Y_2|M}(y_2|-a+b). \end{cases} \quad (3.13)$$

- If T_2 sends $-B$ in the MAC phase, the detection rule is

$$\hat{X}_1 = \begin{cases} +1, & \text{if } f_{Y_2|M}(y_2|a-b) \geq f_{Y_2|M}(y_2|-a-b), \\ -1, & \text{if } f_{Y_2|M}(y_2|a-b) < f_{Y_2|M}(y_2|-a-b). \end{cases} \quad (3.14)$$

The above ML detection eventually gives an optimal decision threshold v_{opt} that results in minimum error probability. However, (3.9) and (3.12) are in complicated forms which may introduce high computational complexity for finding v_{opt} at the destination terminals. We thus try to find a simpler suboptimal decision threshold v_{subopt} in the following. For this, we first take a step back to look at the AWGN-free situation. Since terminal T_1 can transmit $+A$ or $-A$, we consider the two cases separately:

- If T_1 sends $+A$ in the MAC phase, it knows that the relay receives either $Y_R = a + b$ or $Y_R = a - b$. As both values are greater than $w = 0$, the folding operation does not really fold Y_R . The value of Y_1 would be either $h_1\beta(a + b - C)$ or $h_1\beta(a - b - C)$.

Therefore, T_1 makes the following declaration:

$$\hat{X}_2 = \begin{cases} -1, & \text{when } Y_1 = h_1\beta(a - b - C), \\ +1, & \text{when } Y_1 = h_1\beta(a + b - C). \end{cases} \quad (3.15)$$

- If $T1$ sends $-A$ in the MAC phase, it knows that the relay receives either $Y_R = -a + b$ or $Y_R = -a - b$. As both values are less than $w = 0$, the folding operation maps the value $-a + b$ to $a - b$ and the value $-a - b$ to $a + b$. The value of Y_1 would still be either $h_1\beta(a + b - C)$ or $h_1\beta(a - b - C)$. However, $T1$ makes the following declaration:

$$\hat{X}_2 = \begin{cases} +1, & \text{when } Y_1 = h_1\beta(a - b - C), \\ -1, & \text{when } Y_1 = h_1\beta(a + b - C). \end{cases} \quad (3.16)$$

For terminal $T2$, the decision rule is similar:

- If $T2$ sends $+B$ in the MAC phase, it knows that the relay receives either $Y_R = a + b$ or $Y_R = -a + b$. The folding operation maps the value $-a + b$ to $a - b$. The value of Y_2 would be either $h_2\beta(a + b - C)$ or $h_2\beta(a - b - C)$. Therefore, $T2$ declares:

$$\hat{X}_1 = \begin{cases} -1, & \text{when } Y_2 = h_2\beta(a - b - C), \\ +1, & \text{when } Y_2 = h_2\beta(a + b - C). \end{cases} \quad (3.17)$$

- If $T2$ sends $-B$ in the MAC phase, it knows that the relay receives either $Y_R = a - b$ or $Y_R = -a - b$. The folding operation maps the value $-a - b$ to $a + b$. The value of Y_2 would be either $h_2\beta(a + b - C)$ or $h_2\beta(a - b - C)$. Thus, $T2$ declares:

$$\hat{X}_1 = \begin{cases} +1, & \text{when } Y_2 = h_2\beta(a - b - C), \\ -1, & \text{when } Y_2 = h_2\beta(a + b - C). \end{cases} \quad (3.18)$$

Now consider the situation when AWGN is present. Assume that the signal strength is high comparing to noise. Under this situation, at terminal $T1$, the received Y_1 would have a distribution that is approximately the sum of two Gaussian-distributed quantities with different means but the same variance, as illustrated in Fig. 3.3. The typical choice of the decision threshold v_1 for Y_1 is $h_1\beta(a - C)$. That is,

$$\hat{Y}_1 = \begin{cases} h_1\beta(a - b - C), & \text{if } Y_1 < h_1\beta(a - C), \\ h_1\beta(a + b - C), & \text{otherwise.} \end{cases} \quad (3.19)$$

With (3.19) and the detection rule for Y_1 in AWGN-free case, we can summarize the detection rule as:

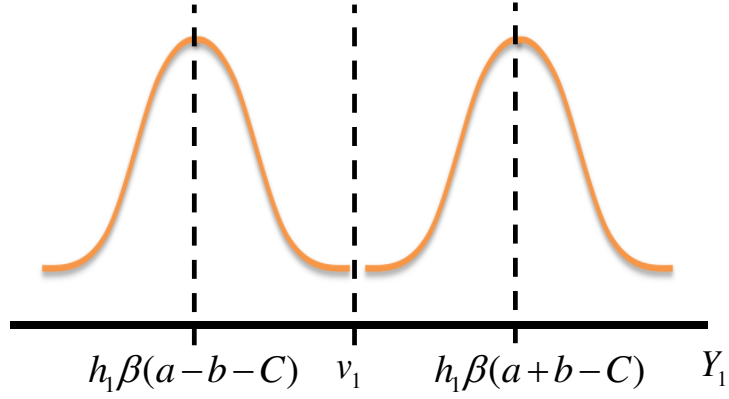


Figure 3.3: Illustration of approximated Y_1 distribution.

- If T_1 sends $+A$ in the MAC phase,

$$\hat{X}_2 = \begin{cases} -1, & \text{if } Y_1 < h_1\beta(a-C), \\ +1, & \text{otherwise.} \end{cases} \quad (3.20)$$

- If T_1 sends $-A$ in the MAC phase,

$$\hat{X}_2 = \begin{cases} +1, & \text{if } Y_1 < h_1\beta(a-C), \\ -1, & \text{otherwise.} \end{cases} \quad (3.21)$$

Similarity for Y_2 , the decision threshold is $v_2 = h_2\beta(a-C)$ and the detection rule is summarized as:

- If T_2 sends $+B$ in the MAC phase,

$$\hat{X}_1 = \begin{cases} -1, & \text{if } Y_2 < h_2\beta(a-C), \\ +1, & \text{otherwise.} \end{cases} \quad (3.22)$$

- If T_2 sends $-B$ in the MAC phase,

$$\hat{X}_1 = \begin{cases} +1, & \text{if } Y_2 < h_2\beta(a-C), \\ -1, & \text{otherwise.} \end{cases} \quad (3.23)$$

3.4 Error Analysis

To start, we note that when $w = 0$, the average error probability at terminal Ti can be written as

$$P_e = \frac{1}{2}\Pr(y_i > v_i | x_1 \neq x_2) + \frac{1}{2}\Pr(y_i < v_i | x_1 = x_2). \quad (3.24)$$

In [6], the author has derived the average error probability for $T1$ when $h_1 = h_2 = 1$ and $A = B = \sqrt{P_s}$ as

$$P_e = \frac{1}{2} + \frac{1}{2} \int_0^{+\infty} (\mathcal{G}(u-2\sqrt{P_s}, \sigma_N^2) + \mathcal{G}(u+2\sqrt{P_s}, \sigma_N^2) - 2\mathcal{G}(u, \sigma_N^2)) \left[\int_{-\infty}^{v_1} \mathcal{G}(y_1 - \beta(u-C), \sigma_Z^2) dy_1 \right] du, \quad (3.25)$$

where $\mathcal{G}(u, \sigma^2) = \frac{1}{\sqrt{2\pi\sigma}} \exp(-\frac{u^2}{2\sigma^2})$.

Experience with MATLAB shows that there is difficulty in carrying out the above double integrations for the FF system, due to the semi-infinite range of integration. So we find an alternative way to calculate the exact error probability of the FF system. In [5], the author provides a method for calculating the error probability of two-dimensional signal constellations. By expressing the distribution of circularly symmetric complex AWGN in polar form, we can simplify the error probability from double integral over an infinite range to a sum of single integrals over finite ranges. This method can be applied here for analyzing the error probability of the FF system and we show how this is done in the following. First, consider the following example, where a signal point S lies on the two-dimensional plane, as shown in Fig. 3.4. The signal is interfered by a zero-mean circularly symmetric AWGN N of variance σ^2 . The decision region for S is the sector bounded by the semi-infinite lines OA and OC ; a decision error happens when Z falls in the sector $\angle AOD$ or sector $\angle DOC$. The probability that Z lies in the sector $\angle AOD$ is

$$P_1 = \int_0^{\pi-\psi_1} d\theta \int_R^\infty p(r, \theta) dr \quad (3.26)$$

where $p(r, \theta)$ is the bivariate Gaussian density function in polar form. Under the assumption that AWGN is circular symmetric, we have

$$p(r, \theta) = \frac{r}{2\pi\sigma} \exp\left(-\frac{r^2}{2\sigma^2}\right) \quad (3.27)$$

Carrying out the integration on r in (3.26) with (3.27), we obtain

$$\begin{aligned} P_1 &= \frac{1}{2\pi} \int_0^{\pi-\psi_1} \exp\left(-\frac{R^2}{2\sigma^2}\right) d\theta \\ &= \frac{1}{2\pi} \int_0^{\pi-\psi_1} \exp\left(-\frac{X_0^2 \sin^2 \psi_1}{2\sigma^2 \sin^2(\theta + \psi_1)}\right) d\theta \\ &= \frac{1}{2\pi} \int_0^{\pi-\psi_1} \exp\left(-\frac{\gamma_s^2 \sin^2 \psi_1}{\sin^2 \phi}\right) d\phi \end{aligned} \quad (3.28)$$

where the second equality holds because $R = \frac{X_0 \sin(\psi_1)}{\sin(\theta + \psi_1)}$ and the third equality results by defining $\gamma_s^2 = \frac{X_0^2}{2\sigma^2}$ and changing variables as $\phi = \pi - (\theta + \psi_1)$. The probability that Z lies in the sector $\angle DOC$ can be similarly derived as

$$P_2 = \frac{1}{2\pi} \int_0^{\pi-\psi_2} \exp\left(-\frac{\gamma_s^2 \sin^2 \psi_2}{\sin^2 \phi}\right) d\phi. \quad (3.29)$$

Therefore, the error probability for S is

$$P_e = P_1 + P_2. \quad (3.30)$$

The above example shows that we can divide the error region into several sectors and represent the probability as a sum of single integrals with finite ranges. Now, we consider the FF bidirectional relay system. Assume that the folding threshold is $w = 0$ and the decision threshold at terminal i is v_i . Also assume that $\sigma_N^2 = \sigma_{Z_i}^2 = \sigma^2$ for simplicity. At $T1$, the decision error on X_2 can be written as

$$\begin{aligned} P_{e_2} &= \Pr(X_1 = +1) [\Pr(X_2 = +1) \Pr(y_1 < v_1 | m = a + b) + \Pr(X_2 = -1) \Pr(y_1 > v_1 | m = a - b)] \\ &\quad + \Pr(X_1 = -1) [\Pr(X_2 = +1) \Pr(y_1 > v_1 | m = -a + b) + \Pr(X_2 = -1) \Pr(y_1 < v_1 | m = -a - b)]. \end{aligned} \quad (3.31)$$

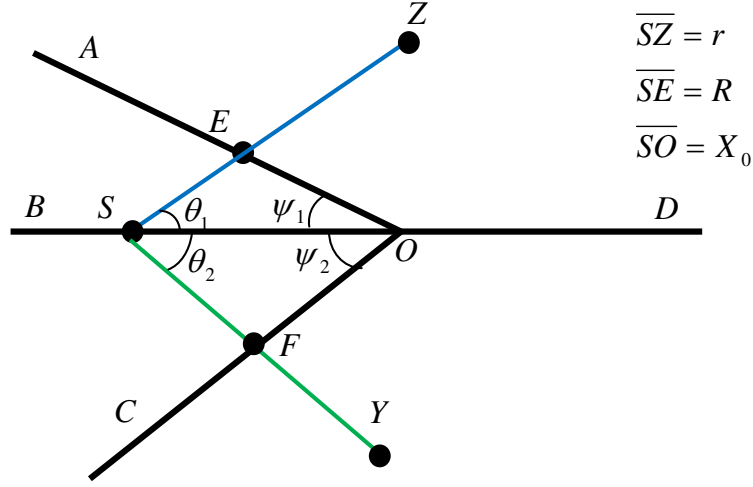


Figure 3.4: A signal point S on two-dimensional plane with circularly symmetric complex AWGN. Sector AOC is the decision region.

With (3.8), we may write the decision boundary $y_1 = v_1$ as

$$\begin{aligned}
 & \begin{cases} h_1\beta(-Y_R - C) + Z_1 = v_1, & \text{if } Y_R < 0, \\ h_1\beta(Y_R - C) + Z_1 = v_1, & \text{otherwise,} \end{cases} \\
 & = \begin{cases} Y_R + \frac{-1}{h_1\beta}Z_1 = \frac{-1}{h_1\beta}v_1 - C, & \text{if } Y_R < 0, \\ Y_R + \frac{1}{h_1\beta}Z_1 = \frac{1}{h_1\beta}v_1 + C, & \text{otherwise.} \end{cases} \quad (3.32)
 \end{aligned}$$

We draw this decision boundary on the signal plane with Y_R and Z_1 being the x-axis and the y-axis, as shown in Fig. 3.5. Now, consider the $m = a + b$ case. The error region is the shaded area shown in Fig. 3.6. Following a similar derivation as in the example, we may obtain the error probability as

$$\begin{aligned}
 \Pr(y_1 < v_1 | m = a + b) &= \frac{1}{2\pi} \int_0^{\pi - (\phi_1 - \phi)} \exp\left(-\frac{\gamma_1^2 \sin^2(\phi_1 - \phi)}{\sin^2\theta}\right) d\theta \\
 &\quad - \frac{1}{2\pi} \int_0^{\pi - (\phi_1 + \phi)} \exp\left(-\frac{\gamma_1^2 \sin^2(\phi_1 + \phi)}{\sin^2\theta}\right) d\theta \quad (3.33)
 \end{aligned}$$

where $\gamma_1^2 = \frac{d_1^2}{2\sigma^2}$. The error region for the $m = a - b$ case is shown in Fig. 3.7, and the error

probability is

$$\begin{aligned} \Pr(y_1 > v_1 | m = a - b) &= \frac{1}{2\pi} \int_0^{\pi - (\phi - \phi_2)} \exp\left(-\frac{\gamma_2^2 \sin^2(\phi - \phi_2)}{\sin^2(\theta)}\right) d\theta \\ &+ \frac{1}{2\pi} \int_0^{\pi - (\phi + \phi_2)} \exp\left(-\frac{\gamma_2^2 \sin^2(\phi + \phi_2)}{\sin^2(\theta)}\right) d\theta \end{aligned} \quad (3.34)$$

with $\gamma_2^2 = \frac{d_2^2}{2\sigma^2}$. Similarly, the error region for $m = -a + b$ and $m = -a - b$ are shown in Figs. 3.8 and 3.9, respectively, and the error probabilities are

$$\begin{aligned} \Pr(y_1 > v_1 | m = -a + b) &= \frac{1}{2\pi} \int_0^{\pi - (\phi - \phi_3)} \exp\left(-\frac{\gamma_3^2 \sin^2(\phi - \phi_3)}{\sin^2(\theta)}\right) d\theta \\ &+ \frac{1}{2\pi} \int_0^{\pi - (\phi + \phi_3)} \exp\left(-\frac{\gamma_3^2 \sin^2(\phi + \phi_3)}{\sin^2(\theta)}\right) d\theta \end{aligned} \quad (3.35)$$

and

$$\begin{aligned} \Pr(y_1 < v_1 | m = -a - b) &= \frac{1}{2\pi} \int_0^{\pi - (\phi_4 - \phi)} \exp\left(-\frac{\gamma_4^2 \sin^2(\phi_4 - \phi)}{\sin^2(\theta)}\right) d\theta \\ &- \frac{1}{2\pi} \int_0^{\pi - (\phi_4 + \phi)} \exp\left(-\frac{\gamma_4^2 \sin^2(\phi_4 + \phi)}{\sin^2(\theta)}\right) d\theta, \end{aligned} \quad (3.36)$$

respectively, with $\gamma_3^2 = \frac{d_3^2}{2\sigma^2}$ and $\gamma_4^2 = \frac{d_4^2}{2\sigma^2}$. Substituting (3.33), (3.34), (3.35) and (3.36) into (3.31) and simplifying, we obtain error probability of X_2 as

$$\begin{aligned} P_{e_2} &= \frac{1}{4\pi} \left[\int_0^{\pi - (\phi_1 - \phi)} \exp\left(-\frac{\gamma_1^2 \sin^2(\phi_1 - \phi)}{\sin^2 \theta}\right) d\theta \right. \\ &+ \int_0^{\pi - (\phi - \phi_2)} \exp\left(-\frac{\gamma_2^2 \sin^2(\phi - \phi_2)}{\sin^2 \theta}\right) d\theta \\ &- \int_0^{\pi - (\phi_1 + \phi)} \exp\left(-\frac{\gamma_1^2 \sin^2(\phi_1 + \phi)}{\sin^2 \theta}\right) d\theta \\ &\left. + \int_0^{\pi - (\phi + \phi_2)} \exp\left(-\frac{\gamma_2^2 \sin^2(\phi + \phi_2)}{\sin^2 \theta}\right) d\theta \right]. \end{aligned} \quad (3.37)$$

One thing to note here is that the above simplification comes from the fact that the folding threshold is at $w = 0$ which produces a symmetric decision region and thus the error probabilities involve the exact same terms when $X_1 = +1$ and $X_1 = -1$. This fact does not hold when $w \neq 0$. For example, if $w = -a$, then the decision boundary is as shown

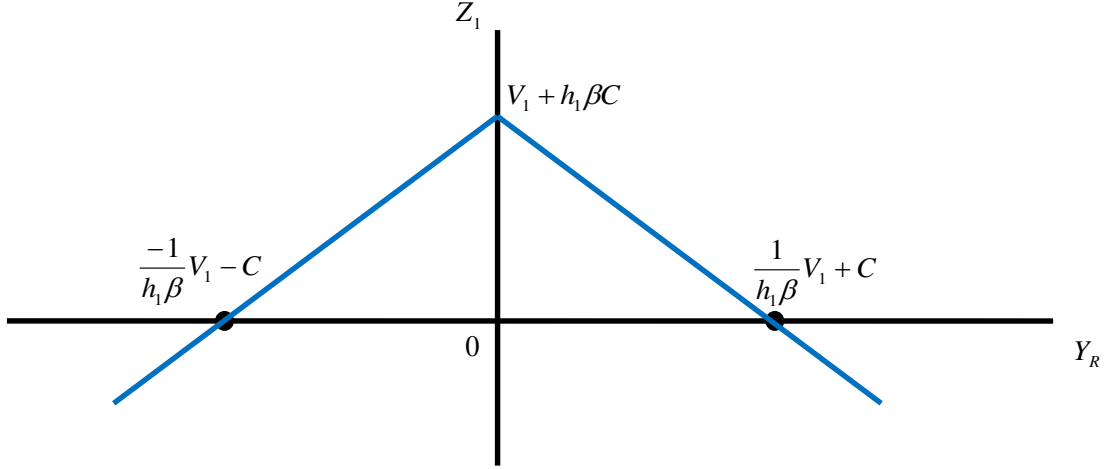


Figure 3.5: The decision boundary of FF system for $T1$.

in Fig. 3.10. It is easy to see from the figure that the error probabilities do not contain the same terms and thus we need to use (3.31) and calculate each term individually using a similar procedure as the one discussed above. For conciseness of this chapter, we leave more detailed discussion on the relation between w and the error probability in the next chapter when we look at high-order modulation system. Nevertheless, we still show the simulation result for the $w = -a$ case along with AF and FF results in the next section.

3.5 Simulation Results

In this section, we present simulation results for uncoded FF bidirectional relay systems. We assume that the instantaneous channel gains are known at the terminals and the relay. We also assume that the variances of AWGNs are $\sigma_N^2 = \sigma_{Z_i}^2 = \sigma^2 = 1$. We define a “weak-signal-to-average noise ratio (WSANR)” as $\frac{B^2}{\sigma^2}$. We set $A = B$ in all simulations and set the relay power constraint to $P_R = B^2$. For comparison, we present the results for AF system, wherein the relay simply amplifies the received signal with proper power scaling. Results for

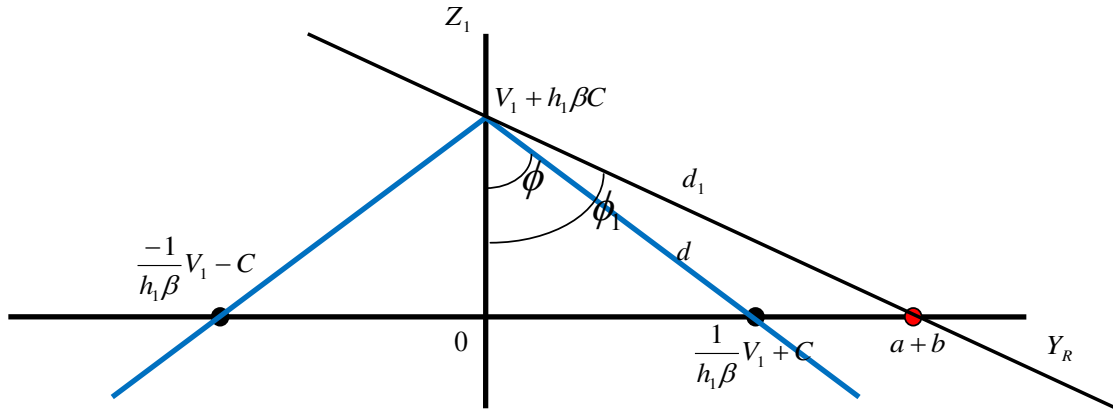


Figure 3.6: Shaded area is the error region when $m = a + b$.

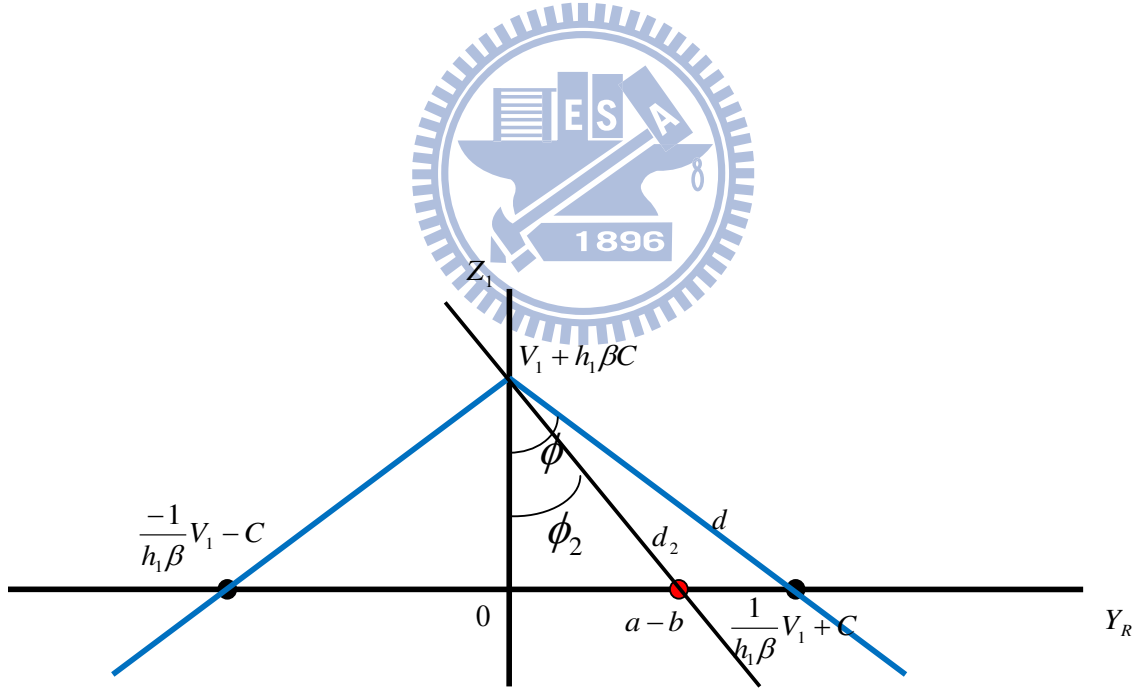


Figure 3.7: Shaded area is the error region when $m = a - b$.

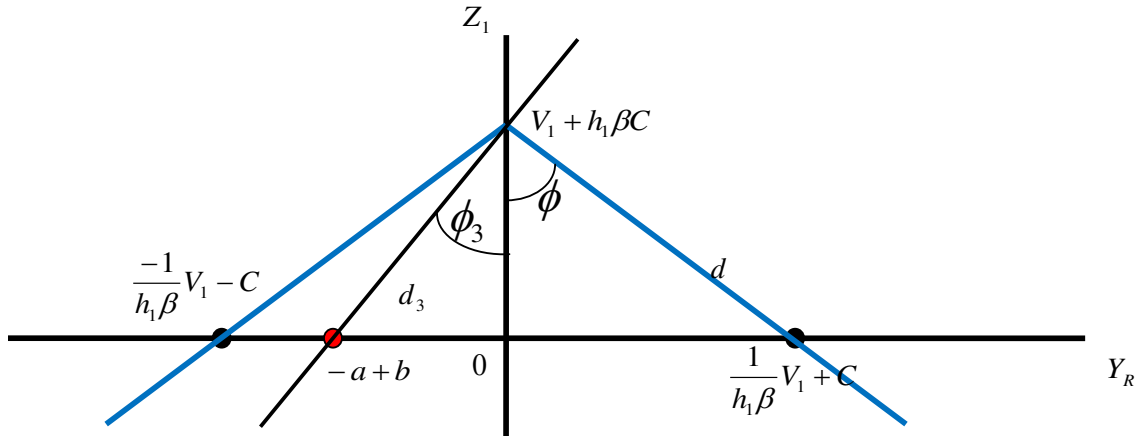


Figure 3.8: Shaded area is the error region when $m = -a + b$.

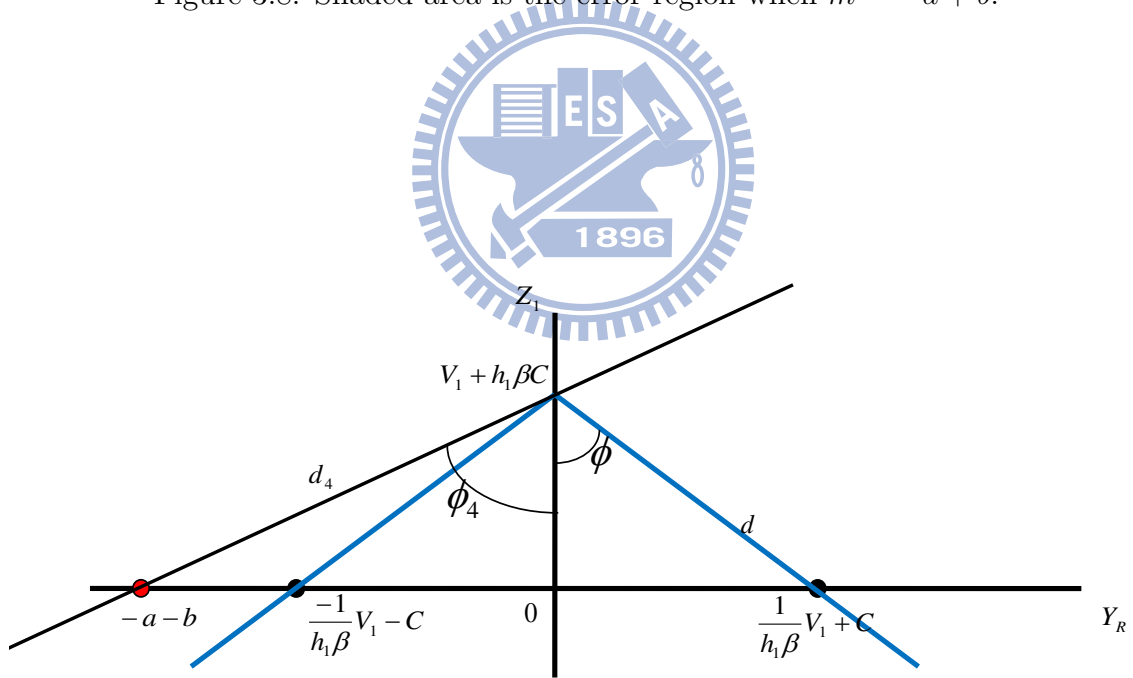


Figure 3.9: Shaded area is the error region when $m = -a - b$.

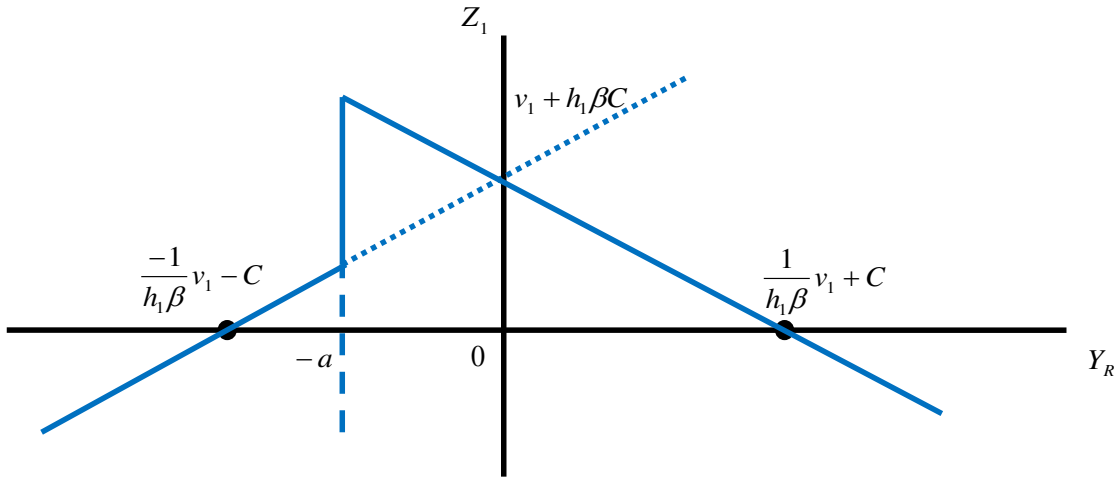


Figure 3.10: The decision boundary of FF system for $T1$ when $w = -a$.

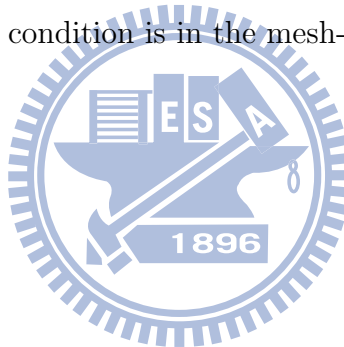
an FF system with folding threshold $w = -a$ are also presented. To distinguish it from the $w = 0$ FF system, we designate the $w = -a$ system as “partial fold-and-forward (PFF).”

Figs. 3.11, 3.12 and 3.13 show the bit error rates (BERs) of all data, of \hat{X}_1 and of \hat{X}_2 , respectively, when $h_1 = 1$ and $h_2 = 1$. The solid lines show the results of Monte Carlo simulation and the dash lines are the analytical results obtained from the two-dimensional error analysis we discussed previously. As we can see from the figures, the FF system provides about 1.5–2 dB gain over the AF system at high WSANR. The PFF system has a very slight performance degradation compared to the FF system; the degradation comes from the fact that PFF only folds part of the signals in the constellation set and thus provides less power saving.

Figs. 3.14, 3.15 and 3.16 show BER results when $h_1 = 1$ and $h_2 = 0.8$. The FF and PFF systems provide about 1 dB overall performance gain. The decrease in performance gain compared to the $h_1 = h_2 = 1$ case mainly comes from the error in \hat{X}_1 . As we can see from Fig. 3.15, the \hat{X}_1 error rates of the three systems are close. The decrease of h_2 degrades the

performance of X_1 detection more in the FF and PFF systems than in the AF system.

Figs. 3.17, 3.18 and 3.19 show BER results when $h_1 = 1$ and $h_2 = 0.5$. The FF system performs slightly better than the AF system at high WSNR, while the PFF system performs worse than the AF system. Looking at Figs. 3.18 and 3.19, we see that this phenomenon is due to that the decrease of h_2 seriously degrades the performance of X_1 detection in the FF and PFF systems. One thing we can conclude from the above results is that the asymmetry of channels in bidirectional relay transmission impacts the best choice of the relay forwarding strategy. When the channels are highly asymmetric, AF may be preferable to FF in performance. To see how relay can determine its forwarding strategy, we plot the overall BERs of FF and AF systems as functions of WSNR and h_2 , for $h_1 = 1$, in Fig. 3.20. The relay should choose AF when the channel condition falls in the solid-color-marked areas and choose FF when the channel condition is in the mesh-marked areas.



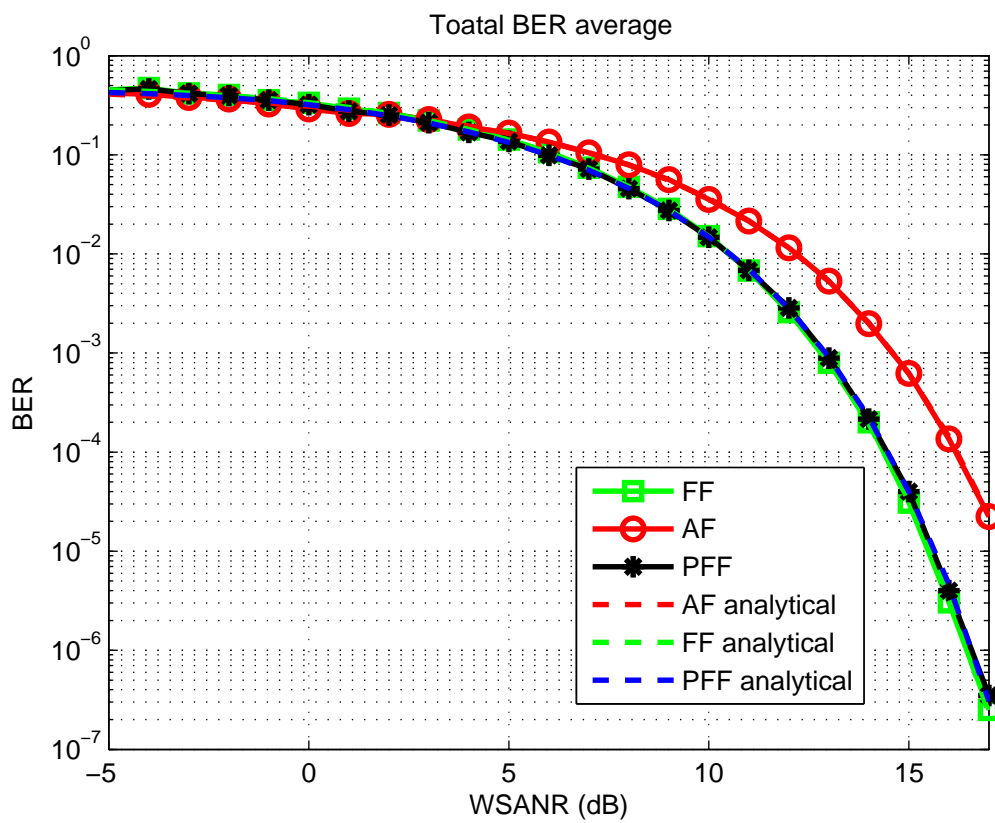


Figure 3.11: Overall BER of FF, AF and PFF systems when $h_1 = 1$ and $h_2 = 1$.

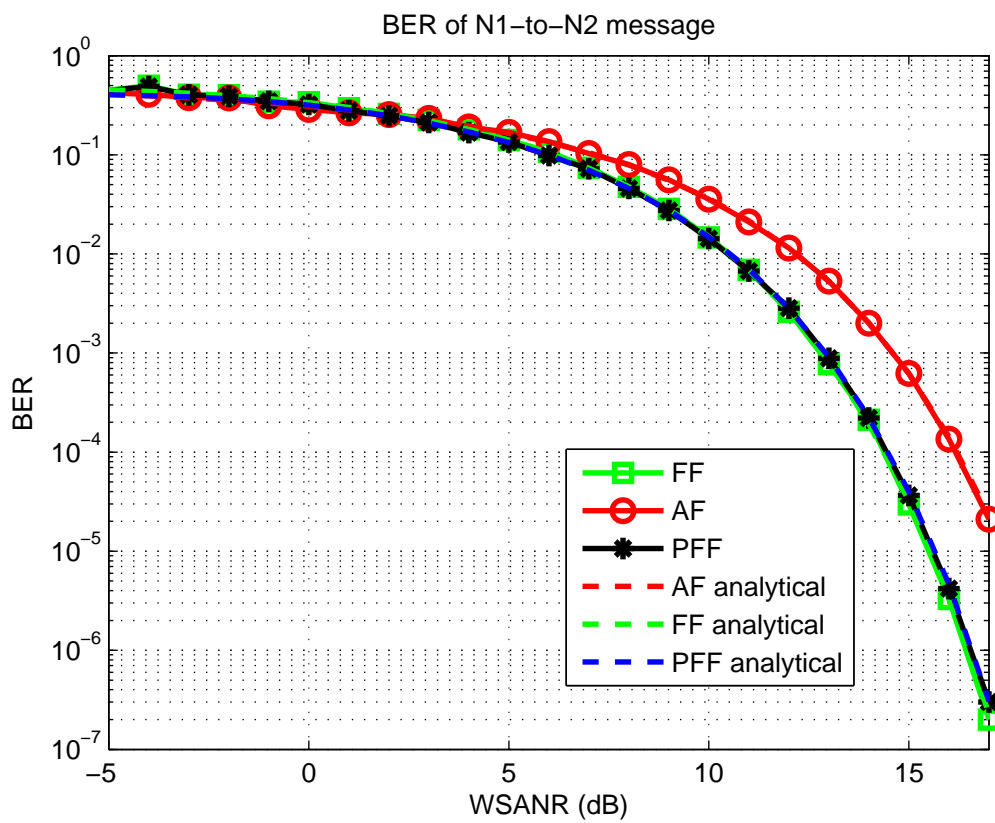


Figure 3.12: BER of T1 data of FF, AF and PFF systems when $h_1 = 1$ and $h_2 = 1$.

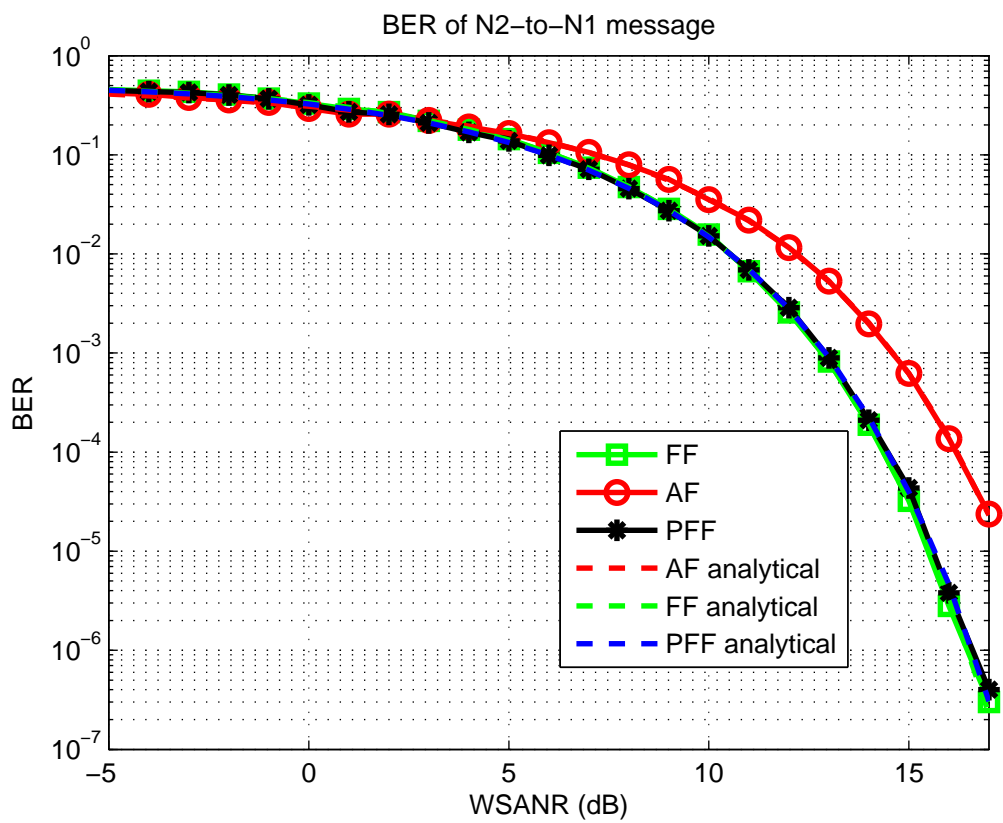


Figure 3.13: BER of T2 data of FF, AF and PFF systems when $h_1 = 1$ and $h_2 = 1$.

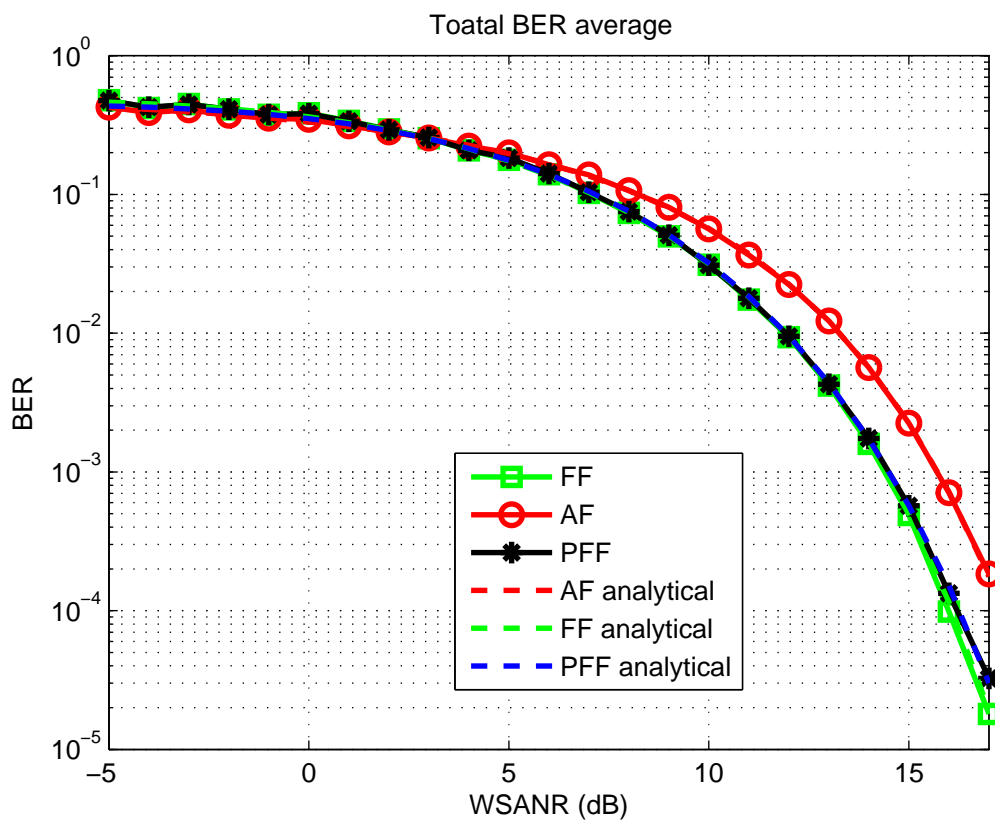


Figure 3.14: Overall BER of FF, AF and PFF systems when $h_1 = 1$ and $h_2 = 0.8$.

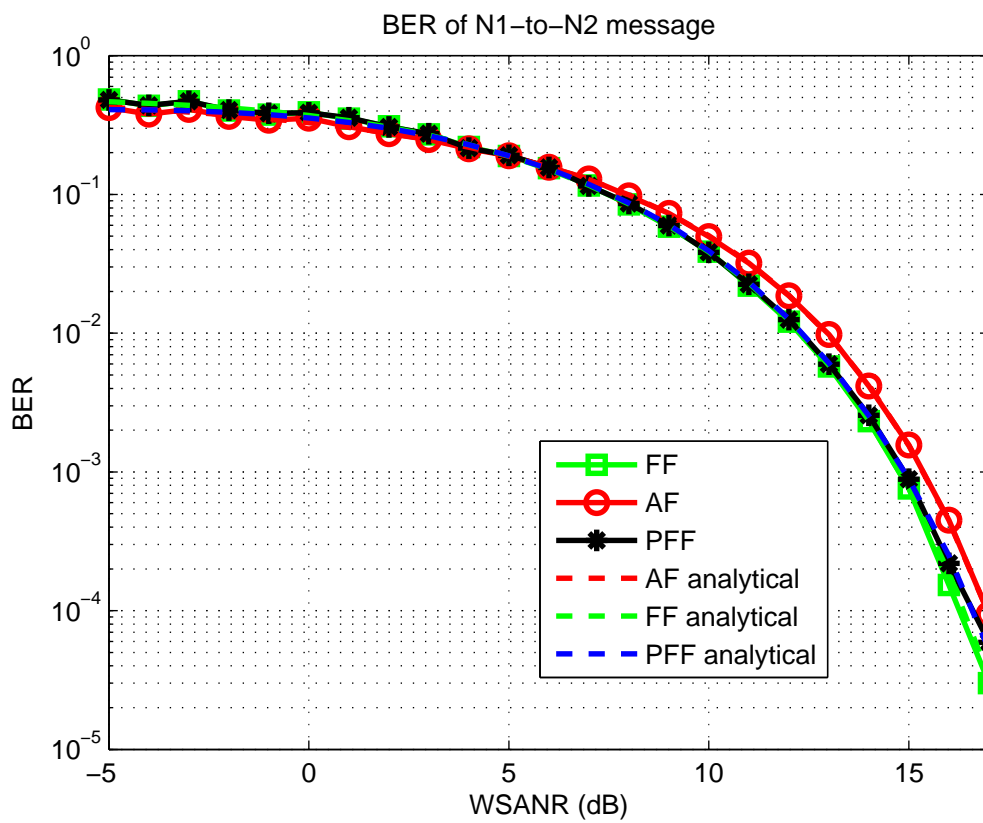


Figure 3.15: BER of T1 data of FF, AF and PFF systems when $h_1 = 1$ and $h_2 = 0.8$.

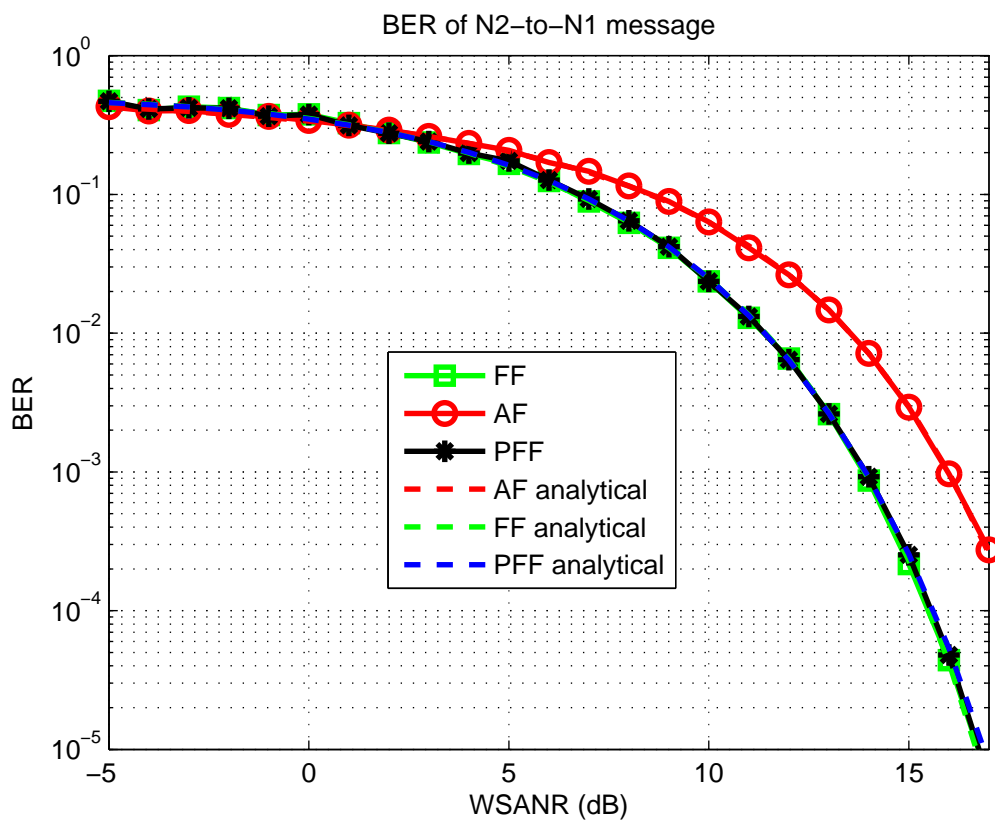


Figure 3.16: BER of T2 data of FF, AF and PFF systems when $h_1 = 1$ and $h_2 = 0.8$.

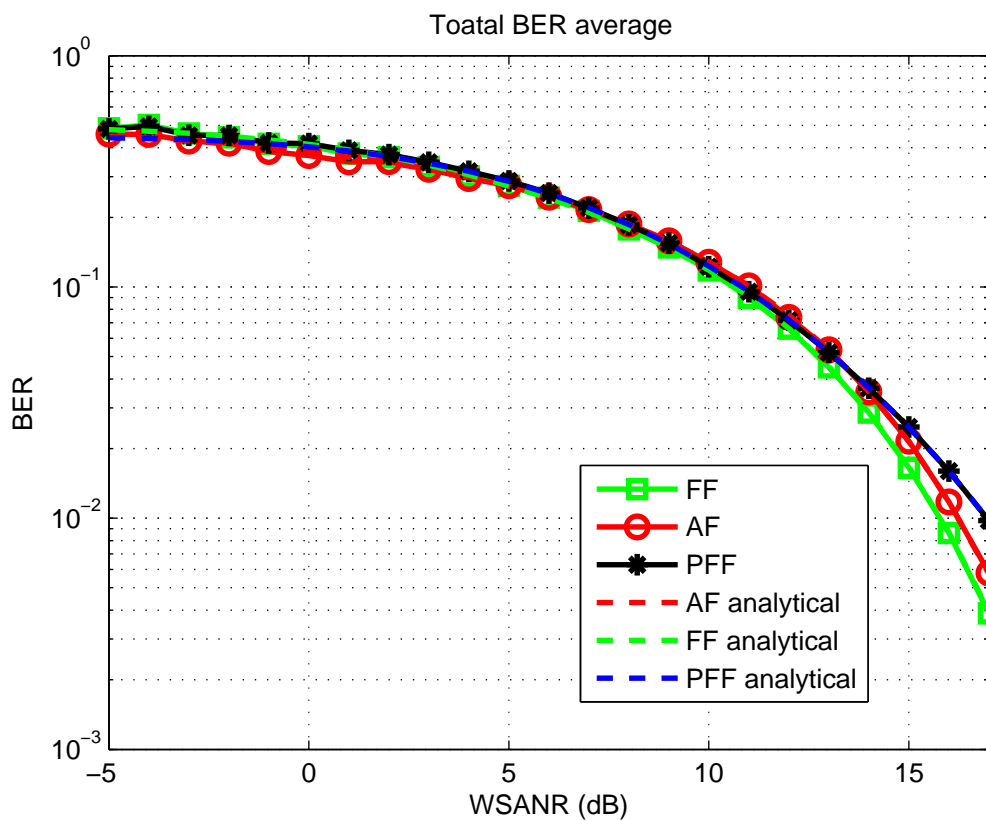


Figure 3.17: Overall BER of FF, AF and PFF systems when $h_1 = 1$ and $h_2 = 0.5$.

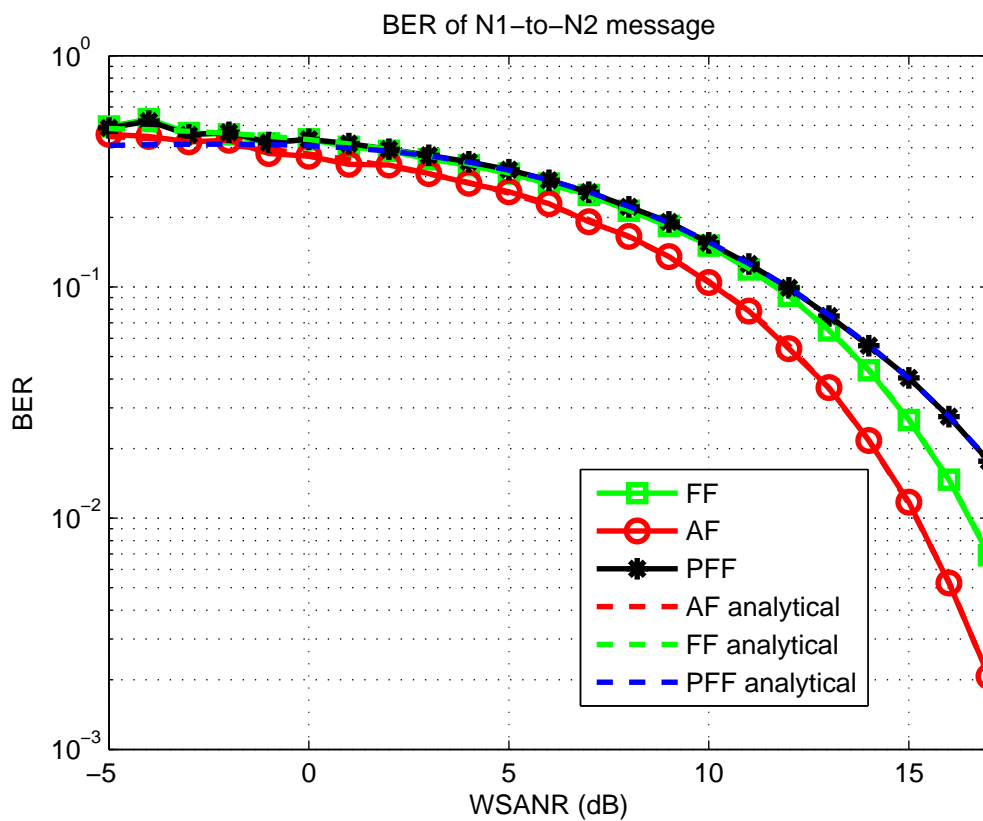


Figure 3.18: BER of T1 data of FF, AF and PFF systems when $h_1 = 1$ and $h_2 = 0.5$.

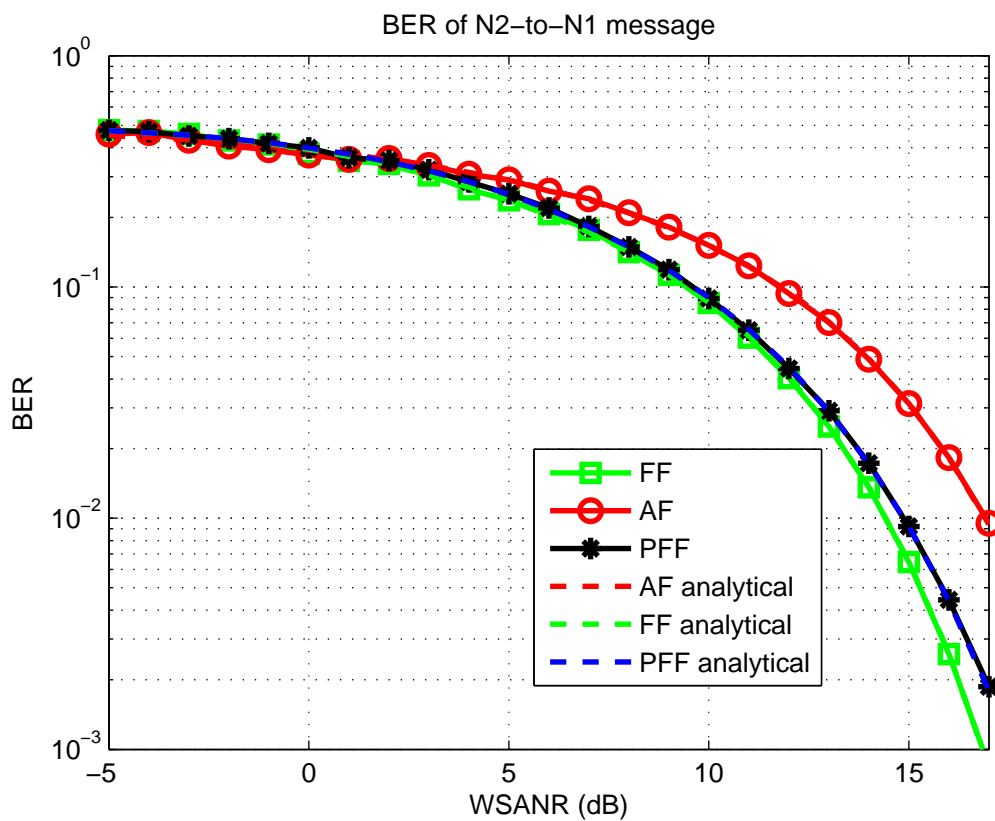


Figure 3.19: BER of T2 data of FF, AF and PFF systems when $h_1 = 1$ and $h_2 = 0.5$.

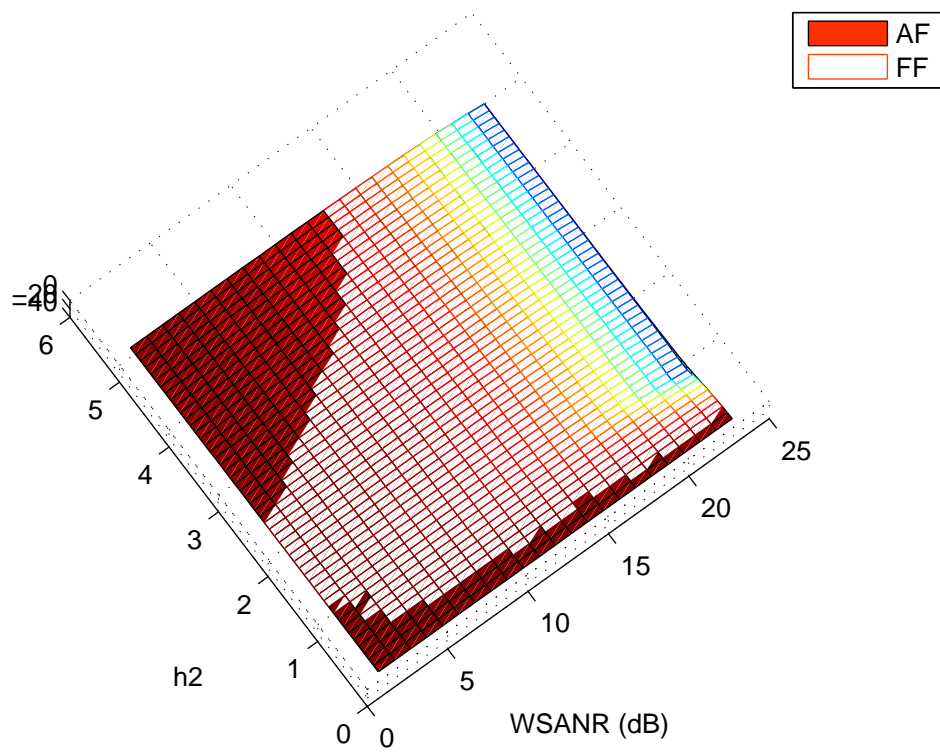


Figure 3.20: Overall BERs of FF and AF systems as functions of WSANR and h_2 .

Chapter 4

Fold-and-Forward Bidirectional Relay System with Higher-Order Modulations

In this chapter, we consider how to apply FF in systems employing higher-order modulation. Two things to note here. The first one is that higher-order modulations, such as QPSK, 16QAM or 64QAM, can be transmitted as two PAM signals, one for the real part and one for the imaginary part. We assume that the channels are perfectly known at the terminals and any phase rotations caused by the channels can be pre-compensated. The second thing to note is that the FF operation can be carried out on each subcarrier in the orthogonal frequency division multiplexing (OFDM) system. The block diagram for OFDM system with FF is shown in Fig. 4.1. As a result, we focus on PAM signals using a single subcarrier and take 4PAM as example. The approach can be generalized to higher PAM constellations. For brevity, we discuss here the “4PAM + BPSK” system, which means that terminal $T1$ transmits 4PAM signal and terminal $T2$ transmits BPSK signal.

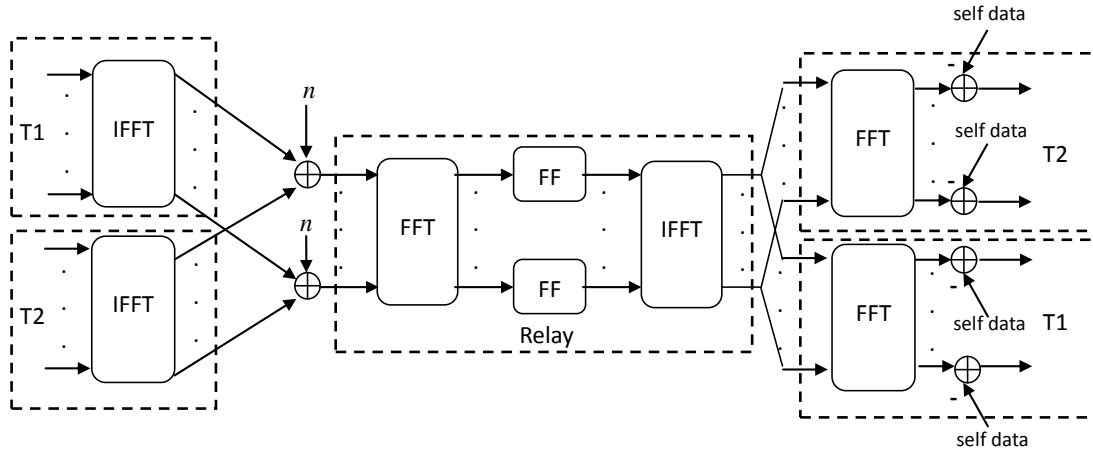


Figure 4.1: Block diagram for OFDM system with FF.

4.1 System Model

The system model is basically the same as discussed in chapter 3, with the only difference that terminal $T1$ transmits 4PAM signal. For convenience, we illustrate of the system model again in Fig. 4.2 and list the definitions of the parameters below.

- X_1 : 4PAM data from terminal $T1$. $X_1 \in \{+1, -1, +3, -3\}$.
- X_2 : BPSK data from terminal $T2$. $X_2 \in \{+1, -1\}$.
- A : amplitude of $T1$'s $+1$ data.
- B : amplitude of $T2$ data.
- X_R : transmitted signal from the relay R .
- Y_1, Y_2, Y_R : received signals at $T1, T2, R$, respectively.
- h_1 : channel gain between $T1$ and R .

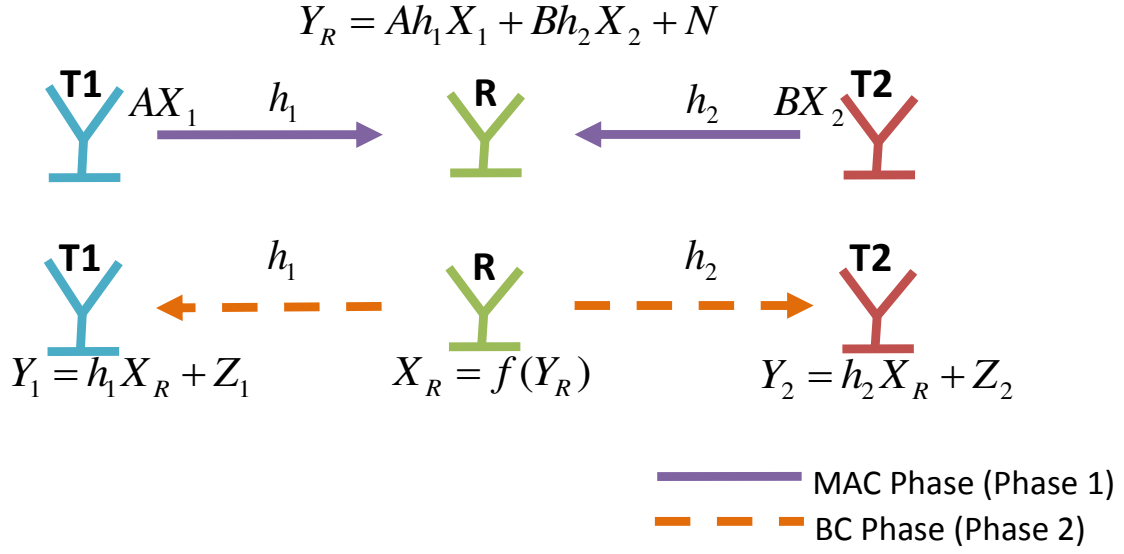


Figure 4.2: System model.

- h_2 : channel gain between $T2$ and R .
- N : AWGN at the relay, with zero mean and variance σ_N^2 .
- Z_1, Z_2 : AWGN at $T1, T2$, respectively, with zero mean and variance σ_Z^2 .
- $a: \triangleq Ah_1$.
- $b: \triangleq Bh_2$.
- $M: \triangleq aX_1 + bX_2$.
- $f(\cdot)$: relay forwarding function, defined as

$$f(u) = \begin{cases} \beta(|u| - C), & \text{if } u < w, \\ \beta(u - C), & \text{otherwise,} \end{cases}$$

with $w \leq 0$ being the folding threshold and C a positive constant.

4.2 Power Scaling

The power scaling factor β can be obtained following the same procedure as in Sec. 3.2. The result is

$$\beta = \sqrt{\frac{P_R}{5a^2 + b^2 + \sigma_N^2 + C^2 - 2CJ}} \quad (4.1)$$

with

$$J = \frac{1}{8}[G(3a + b, w) + G(a + b, w) + G(3a - b, w) + G(a - b, w) \\ + G(-a + b, w) + G(-a - b, w) + G(-3a + b, w) - G(-3a - b, w)]$$

where

$$G(m, w) \triangleq \frac{\sigma_N}{\sqrt{2\pi}} \left[\exp\left(-\frac{(m-w)^2}{2\sigma_N^2}\right) + \exp\left(-\frac{(m+w)^2}{2\sigma_N^2}\right) \right] + m \left[Q\left(-\frac{m-w}{\sigma_N}\right) - Q\left(\frac{m-w}{\sigma_N}\right) \right].$$

4.3 Detection Rule

In this section, we discuss the detection rule at $T2$. The detection rule at $T1$ can be easily obtained from the result in Sec. 3.3, since $T1$ expects to see BPSK signal. For $T2$, recall that the conditional PDF

$$f_{Y_2|M}(y_2|M = m) = \frac{1}{\sqrt{2\pi}\sqrt{h_2^2\beta^2\sigma_N^2 + \sigma_Z^2}} \left[\exp\left(-\frac{(h_2\beta m - (y_2 + C))^2}{2(\sigma_Z^2 + h_2^2\beta^2\sigma_N^2)}\right) Q\left(\frac{w - \frac{\sigma_Z^2 h_2\beta m + h_2^2\beta^2\sigma_N^2(y_2 + C)}{\sigma_Z^2 + h_2^2\beta^2\sigma_N^2}}{\sqrt{\frac{h_2^2\beta^2\sigma_Z^2\sigma_N^2}{\sigma_Z^2 + h_2^2\beta^2\sigma_N^2}}}\right) \right. \\ \left. + \exp\left(-\frac{(h_2\beta m + (y_2 + C))^2}{2(\sigma_Z^2 + h_2^2\beta^2\sigma_N^2)}\right) Q\left(\frac{-w + \frac{\sigma_Z^2 h_2\beta m - h_2^2\beta^2\sigma_N^2(y_2 + C)}{\sigma_Z^2 + h_2^2\beta^2\sigma_N^2}}{\sqrt{\frac{h_2^2\beta^2\sigma_Z^2\sigma_N^2}{\sigma_Z^2 + h_2^2\beta^2\sigma_N^2}}}\right) \right]. \quad (4.2)$$

The ML detection rule can be applied to get the following:

- If $T2$ sends $+B$ in the MAC phase, then $m \in S^+ = \{3a + b, a + b, -a + b, -3a + b\}$,

and the detection rule is:

$$\hat{X}_1 = \begin{cases} -3, & \text{if } f_{Y_2|M}(y_2|m) \text{ is maximum for } m = -3a + b, \\ -1, & \text{if } f_{Y_2|M}(y_2|m) \text{ is maximum for } m = -a + b, \\ +1, & \text{if } f_{Y_2|M}(y_2|m) \text{ is maximum for } m = a + b, \\ +3, & \text{if } f_{Y_2|M}(y_2|m) \text{ is maximum for } m = 3a + b. \end{cases} \quad (4.3)$$

- If T_2 sends $-B$ in the MAC phase, then $m \in S^- = \{3a - b, a - b, -a - b, -3a - b\}$,

and the detection rule is:

$$\hat{X}_1 = \begin{cases} -3, & \text{if } f_{Y_2|M}(y_2|m) \text{ is maximum for } m = -3a - b, \\ -1, & \text{if } f_{Y_2|M}(y_2|m) \text{ is maximum for } m = -a - b, \\ +1, & \text{if } f_{Y_2|M}(y_2|m) \text{ is maximum for } m = a - b, \\ +3, & \text{if } f_{Y_2|M}(y_2|m) \text{ is maximum for } m = 3a - b. \end{cases} \quad (4.4)$$

Considering the high SNR situation, we may again simplify the detection rule. Note that the detection rule depends on the folding threshold w , since different w values result in different signal distributions at T_2 . Take the $w = -2a$ case for example, if T_2 sends $+B$ in the MAC phase, then it knows that in the BC phase it will see a signal with distribution of the shape illustrated in Fig. 4.3. The four peaks happen at $Y_2 = h_2\beta(-a + b - C)$, $h_2\beta(a + b - C)$, $h_2\beta(3a - b - C)$, and $h_2\beta(3a + b - C)$. The decision thresholds are therefore chosen as $v_1 = h_2\beta(b - C)$, $v_2 = h_2\beta(2a - C)$, and $v_3 = h_2\beta(3a - C)$.

If T_2 sends $-B$ in the MAC phase, then it will see a signal with distribution of the shape illustrated in Fig. 4.4. The four peaks happen at $Y_2 = h_2\beta(-a - b - C)$, $h_2\beta(a - b - C)$, $h_2\beta(3a - b - C)$, and $h_2\beta(3a + b - C)$. The decision thresholds are therefore chosen as $v_1 = h_2\beta(-b - C)$, $v_2 = h_2\beta(2a - b - C)$, and $v_3 = h_2\beta(3a - C)$.

The decision thresholds and the detection rule for other choice of w can be derived by the same procedure. At the end of this section, we summarize the simplified detection rules for three typical w values, i.e., $w = 0$, $w = -2a$ and $w = -3a$. Note that the value of C is different for each different w value.

When the folding threshold is $w = 0$, the detection rule is simplified as follows:

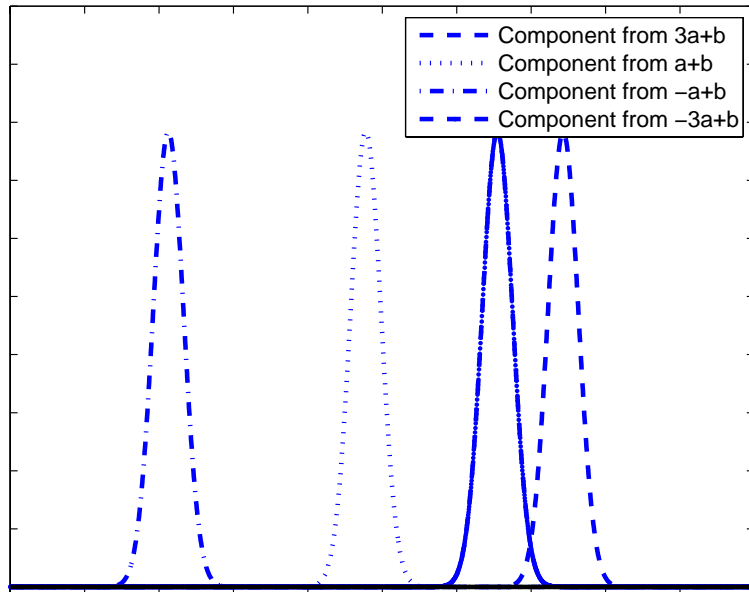


Figure 4.3: Signal distribution seen at $T2$ when $w = -2a$ and $T2$ sends $+B$.

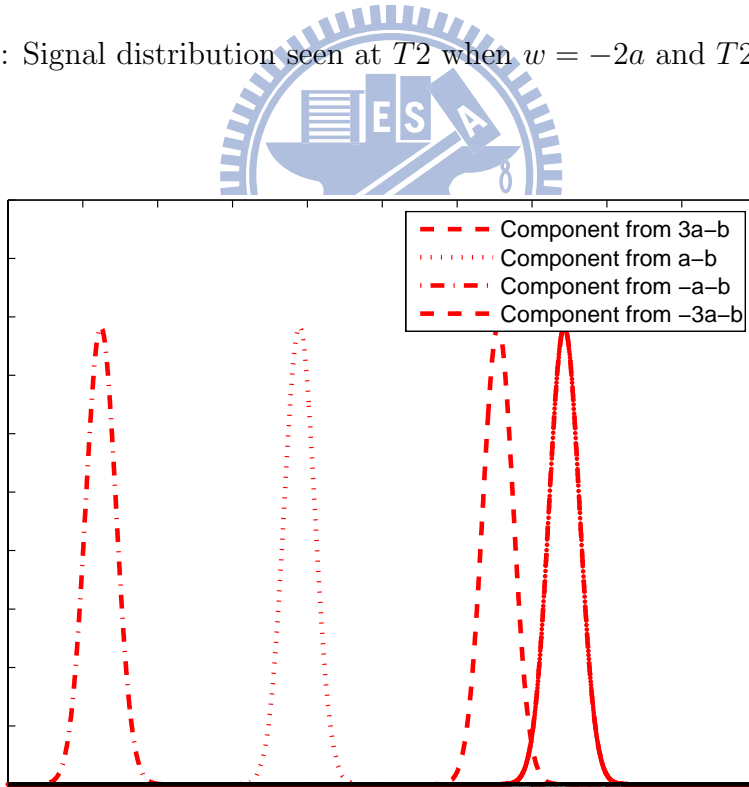


Figure 4.4: Signal distribution seen at $T2$ when $w = -2a$ and $T2$ sends $-B$.

- If T_2 sends $+B$ in the MAC phase,

$$\hat{X}_1 = \begin{cases} -1, & \text{if } Y_2 < h_2\beta(a - C), \\ +1, & \text{if } h_2\beta(a - C) \leq Y_2 < h_2\beta(2a - C), \\ -3, & \text{if } h_2\beta(2a - C) \leq Y_2 < h_2\beta(3a - C), \\ +3, & \text{otherwise.} \end{cases} \quad (4.5)$$

- If T_2 sends $-B$ in the MAC phase,

$$\hat{X}_1 = \begin{cases} +1, & \text{if } Y_2 < h_2\beta(a - C), \\ -1, & \text{if } h_2\beta(a - C) \leq Y_2 < h_2\beta(2a - C), \\ +3, & \text{if } h_2\beta(2a - C) \leq Y_2 < h_2\beta(3a - C), \\ -3, & \text{otherwise.} \end{cases} \quad (4.6)$$

When the folding threshold is $w = -2a$, the simplified detection rule is:

- If T_2 sends $+B$ in the MAC phase,

$$\hat{X}_1 = \begin{cases} -1, & \text{if } Y_2 < h_2\beta(b - C), \\ +1, & \text{if } h_2\beta(b - C) \leq Y_2 < h_2\beta(2a - C), \\ -3, & \text{if } h_2\beta(2a - C) \leq Y_2 < h_2\beta(3a - C), \\ +3, & \text{otherwise.} \end{cases} \quad (4.7)$$

- If T_2 sends $-B$ in the MAC phase,

$$\hat{X}_1 = \begin{cases} -1, & \text{if } Y_2 < h_2\beta(-b - C), \\ +1, & \text{if } h_2\beta(-b - C) \leq Y_2 < h_2\beta(2a - b - C), \\ +3, & \text{if } h_2\beta(2a - b - C) \leq Y_2 < h_2\beta(3a - C), \\ -3, & \text{otherwise.} \end{cases} \quad (4.8)$$

When the folding threshold is $w = -3a$, the simplified detection rule is:

- If T_2 sends $+B$ in the MAC phase,

$$\hat{X}_1 = \begin{cases} -3, & \text{if } Y_2 < h_2\beta(-2a + b - C), \\ -1, & \text{if } h_2\beta(-2a + b - C) \leq Y_2 < h_2\beta(b - C), \\ +1, & \text{if } h_2\beta(b - C) \leq Y_2 < h_2\beta(2a + b - C), \\ +3, & \text{otherwise.} \end{cases} \quad (4.9)$$

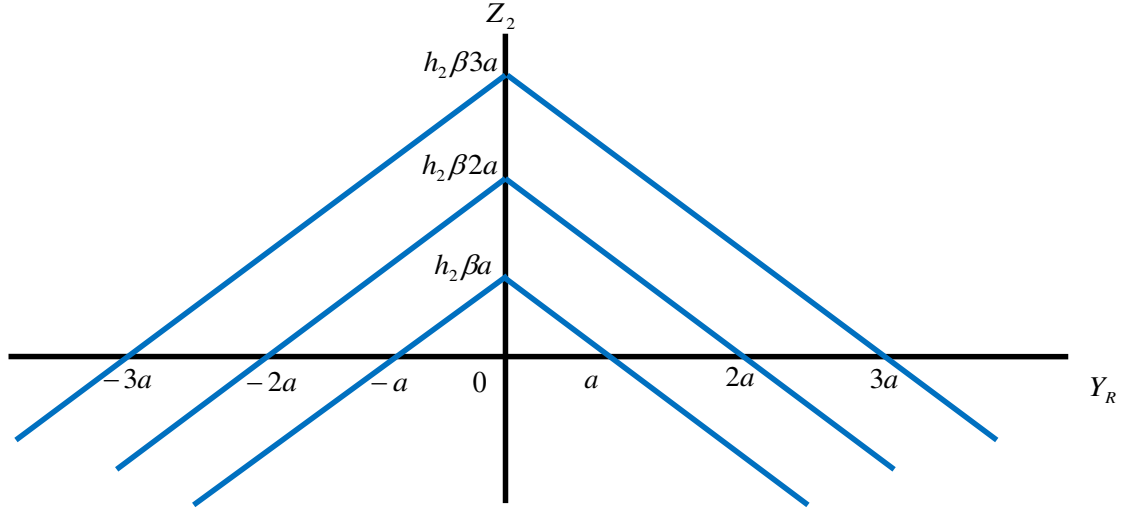


Figure 4.5: Decision boundaries of the 4PAM+BPSK FF system for T_2 when $w = 0$.

- If T_2 sends $-B$ in the MAC phase,

$$\hat{X}_1 = \begin{cases} -1, & \text{if } Y_2 < h_2\beta(-b - C), \\ +1, & \text{if } h_2\beta(-b - C) \leq Y_2 < h_2\beta(2a - b - C), \\ +3, & \text{if } h_2\beta(2a - b - C) \leq Y_2 < h_2\beta(3a - C), \\ -3, & \text{otherwise.} \end{cases} \quad (4.10)$$

4.4 Error Analysis

The symbol error performance of FF in the 4PAM + BPSK system can be derived using the two dimensional signal plane method we introduced in Sec. 3.4. Note that at T_2 , the decision region is of the shape shown in Fig. 4.5 for $w = 0$ and Fig. 4.6 for $w \neq 0$.

We give some remarks on the folding threshold w here. It may be not so obvious why we would have such a parameter in the system, since it seems that we only need to choose $w = 0$ to fold half of the signal plane to the other half as in the BPSK + BPSK case. However, the reason becomes clear when we consider higher-order modulations. In systems with higher-order modulations, the combining of two signals may result in constellation overlapping. If

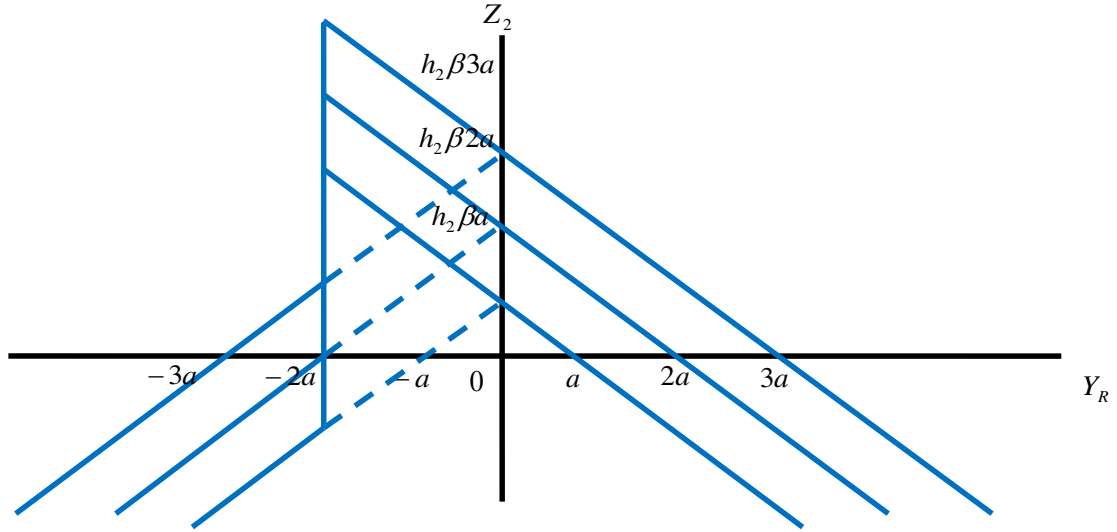
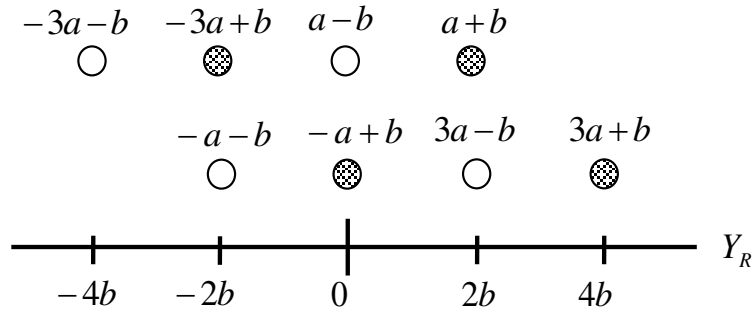
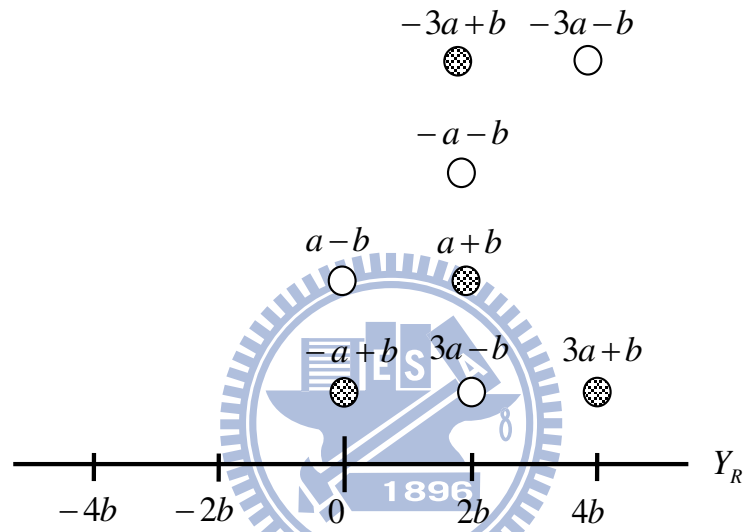


Figure 4.6: Decision boundaries of the 4PAM+BPSK FF system for T_2 when $w \neq 0$.

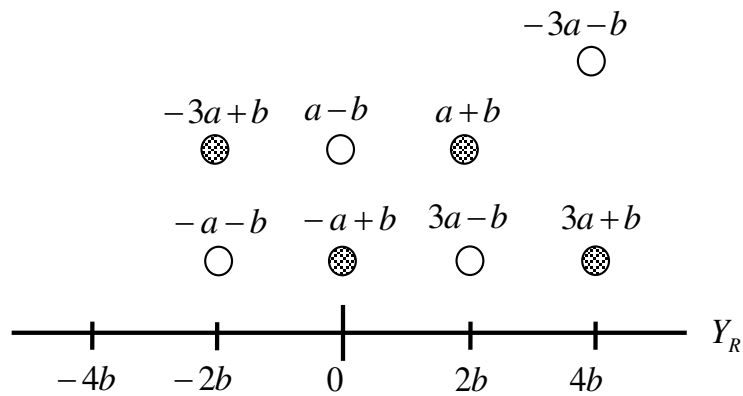
the overlapped constellation is folded again, there will be ambiguity such that the terminal cannot distinguish the desired data. To illustrate this problem, consider the case where $a = b$ in absence of AWGN. As shown in Fig. 4.7(a), the relay receives a signal value in the set $\{-4b, -2b, 0, +2b, +4b\}$ with probability $\{\frac{1}{8}, \frac{1}{4}, \frac{1}{4}, \frac{1}{4}, \frac{1}{8}\}$. The value $-2b$ may come from $-a - b$ or $-3a + b$ and the value $+2b$ may come from $a + b$ or $3a - b$. If the folding threshold is set as $w = 0$, as shown in Fig. 4.7(b), the value $-2b$ will be folded to $+2b$. At T_2 , when it sees the received value being $+2b$, it cannot distinguish the real T_1 data: if T_2 transmits $+B$, T_1 data may be $-3A$ or A ; if T_2 transmits $-B$, T_1 data may be $3A$ or $-A$. This ambiguity limits the performance of the FF system and can be avoided by selecting a different folding threshold. For instance, in the above example, if we choose a folding threshold $w = -3a$, as shown in Fig. 4.7(c), then only the signal value $-4b$ will be folded to $+4b$ and thus the ambiguity is avoided. The conclusion is that the performance of the FF operation depends heavily on the channel conditions, especially with using higher-order modulations. Thus we



(a) Value set before folding.



(b) Value set after $w = 0$ folding.



(c) Value set after $w = -3a$ folding.

Figure 4.7: Relay signal value sets of the 4PAM+BPSK FF system when $a = b$ in absence of AWGN.

need to choose a proper forwarding strategy based on the channel conditions.

4.5 Simulation Results

In this section, we present the simulation results for uncoded FF bidirectional relaying with $T1$ transmitting 4PAM signals and $T2$ transmitting BPSK signals. We also present the results for AF relaying, and that of PFF relaying whose folding threshold is $w = -3a$. We assume that the variances of AWGNs are $\sigma_N^2 = \sigma_{Z_i}^2 = \sigma^2 = 1$. We set $A = B$ in all simulations and set the relay power constraint as $P_R = B^2$.

Figs. 4.8, 4.9 and 4.10 show the symbol error rates (SERs) of all data, of \hat{X}_1 and of \hat{X}_2 , respectively, when $h_1 = 1$ and $h_2 = 1$. The SER of all data is given by $\frac{\Pr(\hat{X}_1 \neq X_1) + \Pr(\hat{X}_2 \neq X_2)}{2}$. As we can see from the figures, the FF system experiences an error floor phenomenon which results from the ambiguity problem that we mentioned previously. The PFF system, with proper choice of the w value, avoids the ambiguity and provides about 0.5–1 dB gain over the AF system.

Figs. 4.11, 4.12 and 4.13 show the SERs of all data, of \hat{X}_1 and of \hat{X}_2 , respectively, when $h_1 = 1$ and $h_2 = 0.8$. We observe that the FF system still experiences performance degradation due to X_1 detection error. This is because that the signal constellations, though not overlapped, are quite close and still incur ambiguity to some extent, as shown in Fig. 4.14. We also notice that the PFF system also experiences some performance degradation due to the asymmetric channel.

Figs. 4.15, 4.16 and 4.17 show the SER of all data, of \hat{X}_1 and \hat{X}_2 , respectively, when $h_1 = 1$ and $h_2 = 0.5$. As shown in Fig. 4.18, now the FF system does not experience ambiguity and thus is able to provide about 1–1.5 dB of performance gain over the AF system. We also see that the channel asymmetry causes more harm on the PFF system than

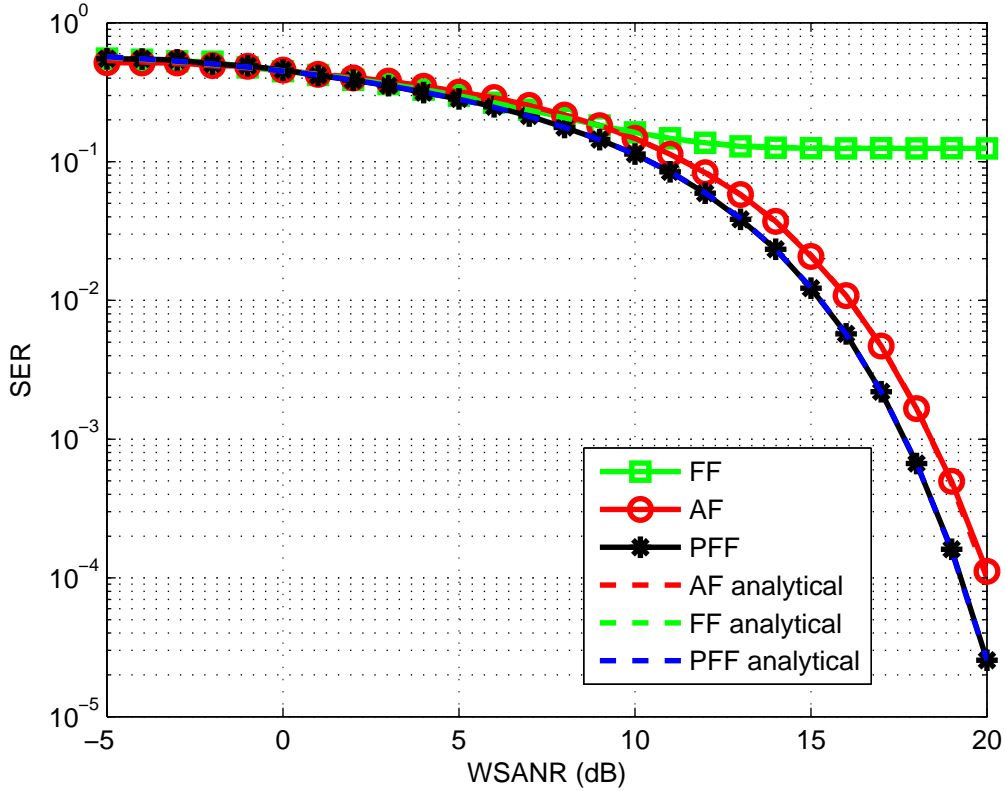


Figure 4.8: Overall SER of FF, AF and PFF systems when $h_1 = 1$ and $h_2 = 1$.

on the AF system, which results in worse overall SER for the PFF system.

We give a concluding remark here. In high-order modulated bidirectional relay system, the design of forwarding strategy is more sophisticated. We need to consider not only the channel conditions but also the signal constellation to avoid decoding ambiguity. To provide better SER performance, the bidirectional relay should be designed to sense the asymmetry of channel and able to switch between AF, FF and PFF.

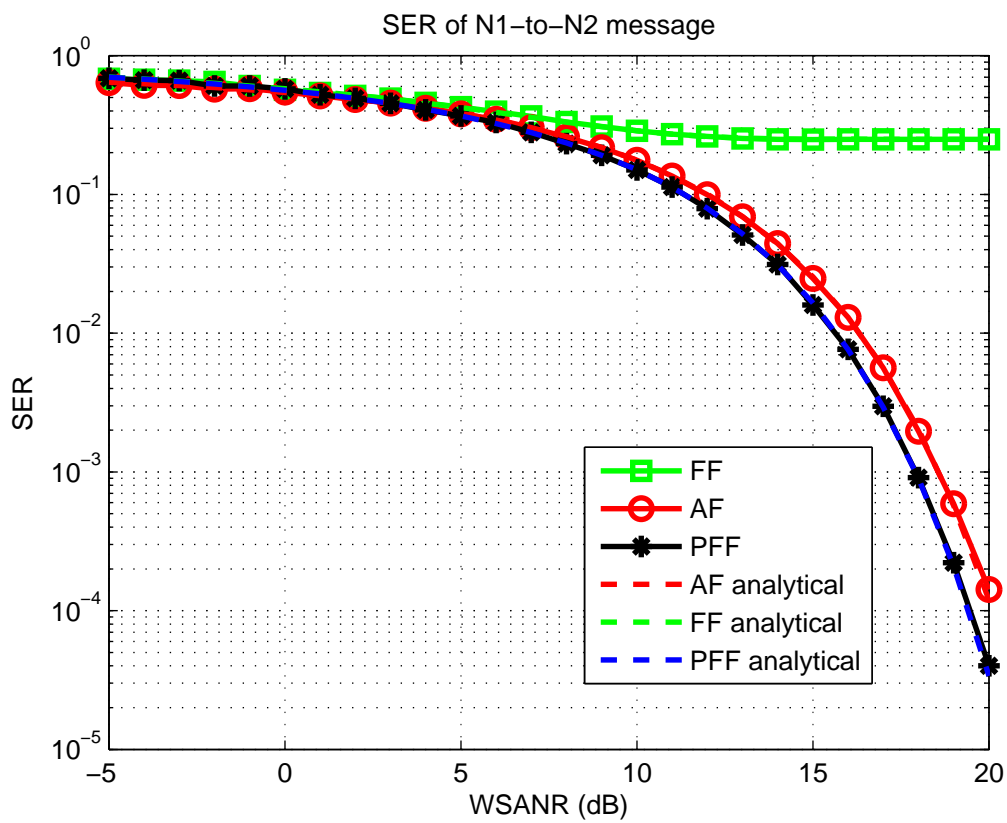


Figure 4.9: SER of T1 data of FF, AF and PFF systems when $h_1 = 1$ and $h_2 = 1$.

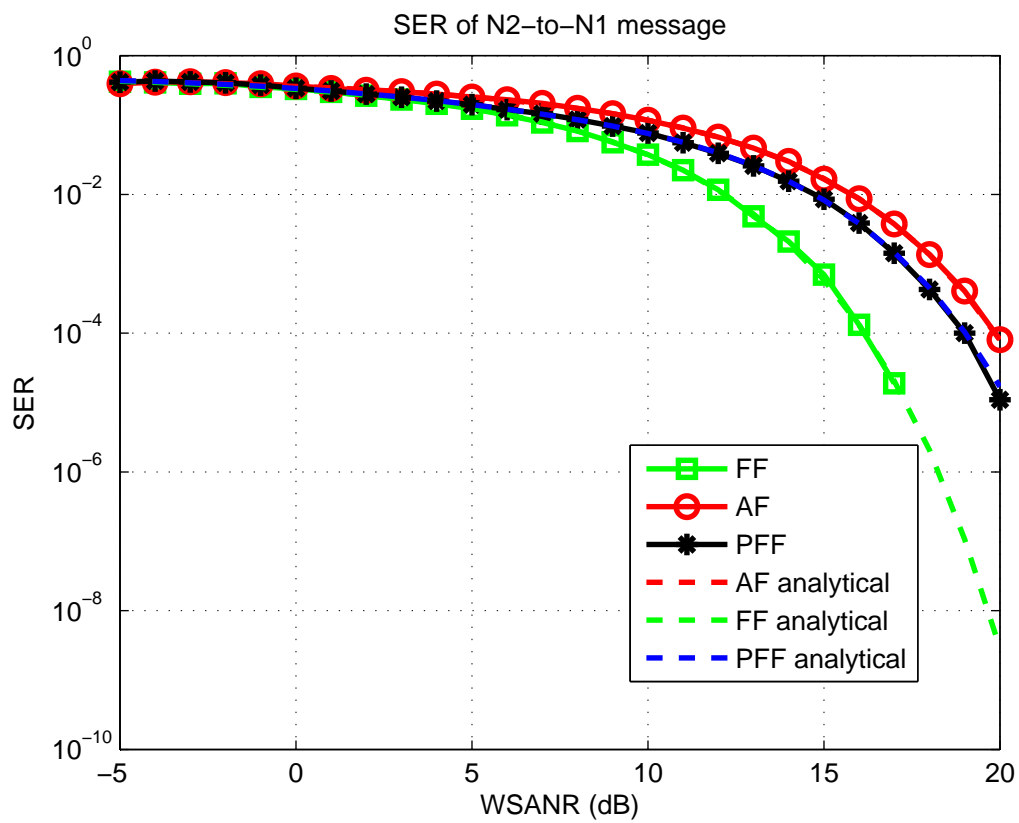


Figure 4.10: SER of T2 data of FF, AF and PFF systems when $h_1 = 1$ and $h_2 = 1$.

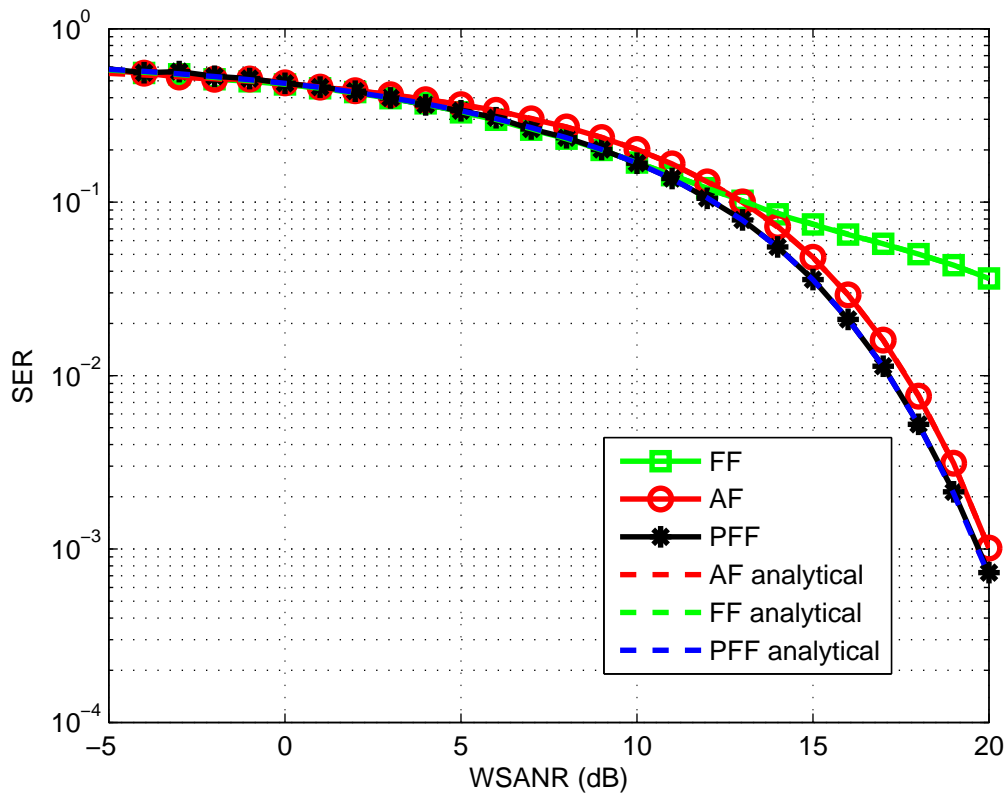


Figure 4.11: Overall SER of FF, AF and PFF systems when $h_1 = 1$ and $h_2 = 0.8$.

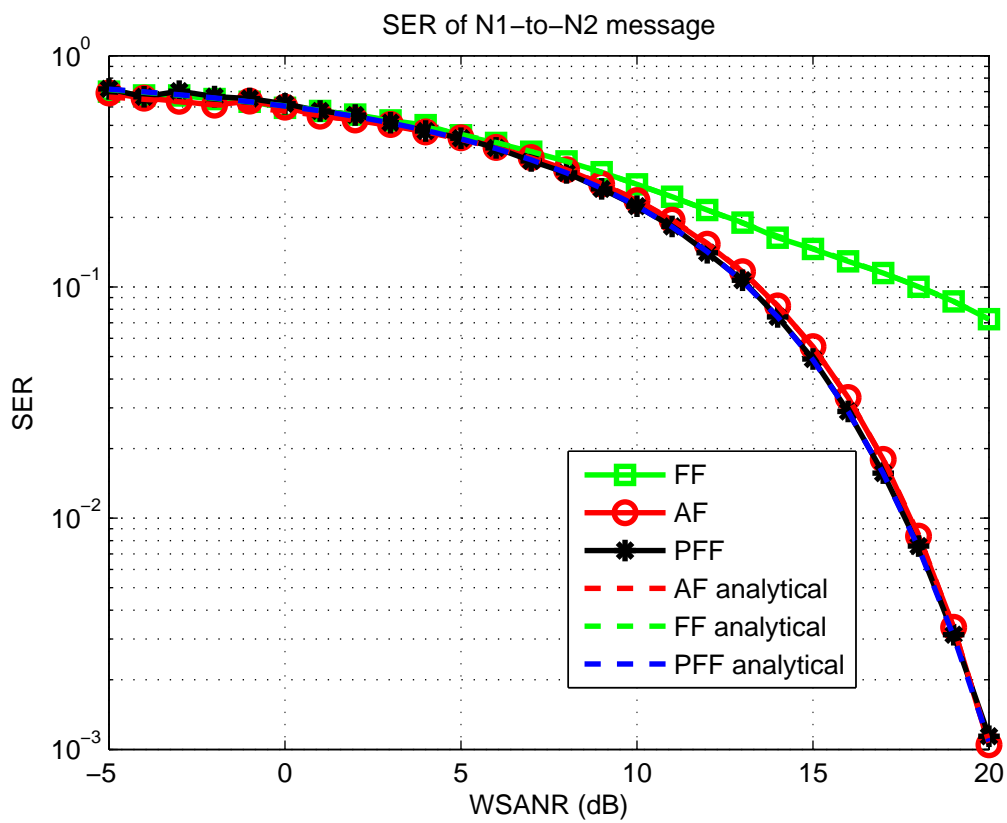


Figure 4.12: SER of T1 data of FF, AF and PFF systems when $h_1 = 1$ and $h_2 = 0.8$.

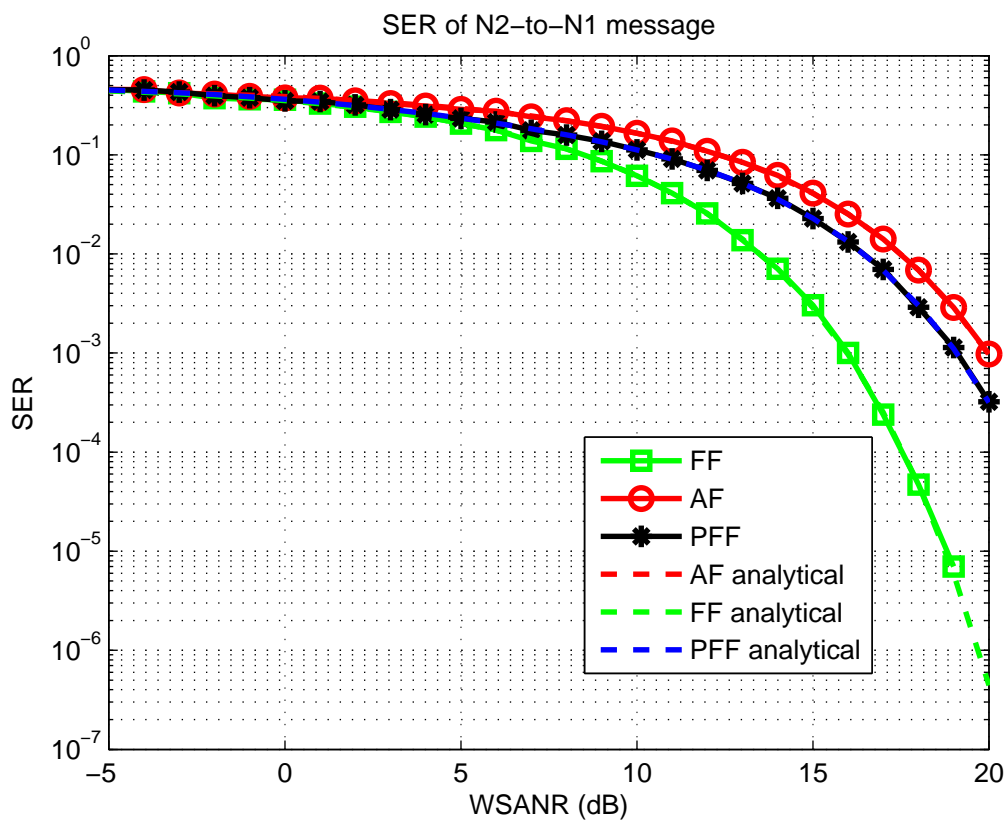


Figure 4.13: SER of T2 data of FF, AF and PFF systems when $h_1 = 1$ and $h_2 = 0.8$.

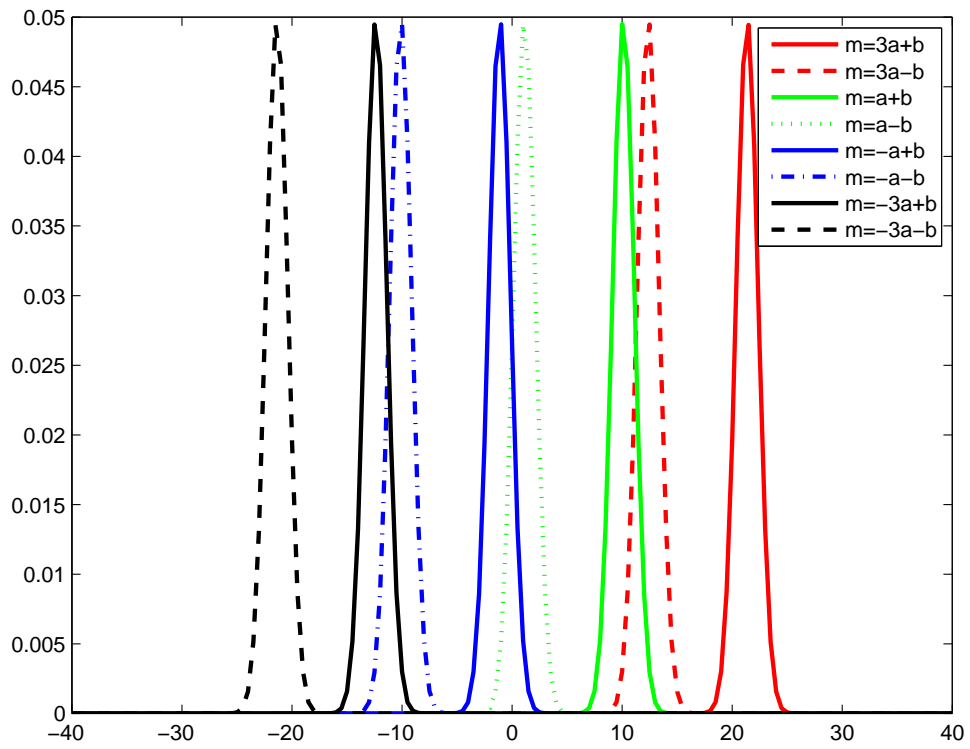


Figure 4.14: Signal distribution of Y_R when $h_1 = 1$ and $h_2 = 0.8$.

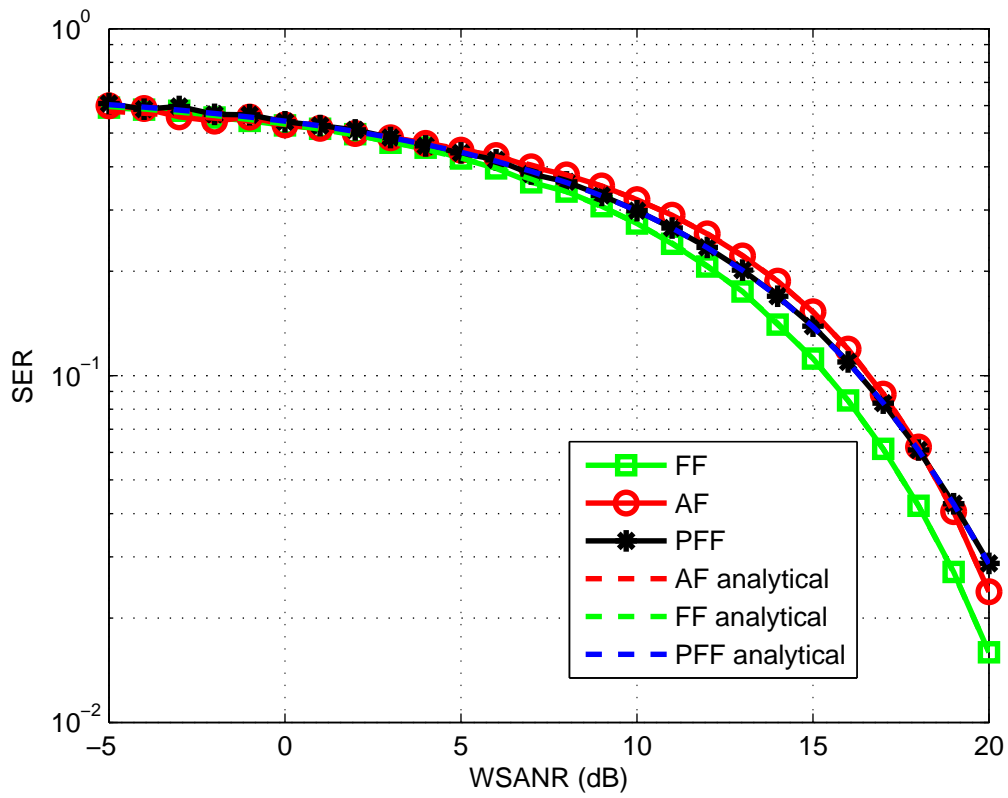


Figure 4.15: Overall SER of FF, AF and PFF systems when $h_1 = 1$ and $h_2 = 0.5$.

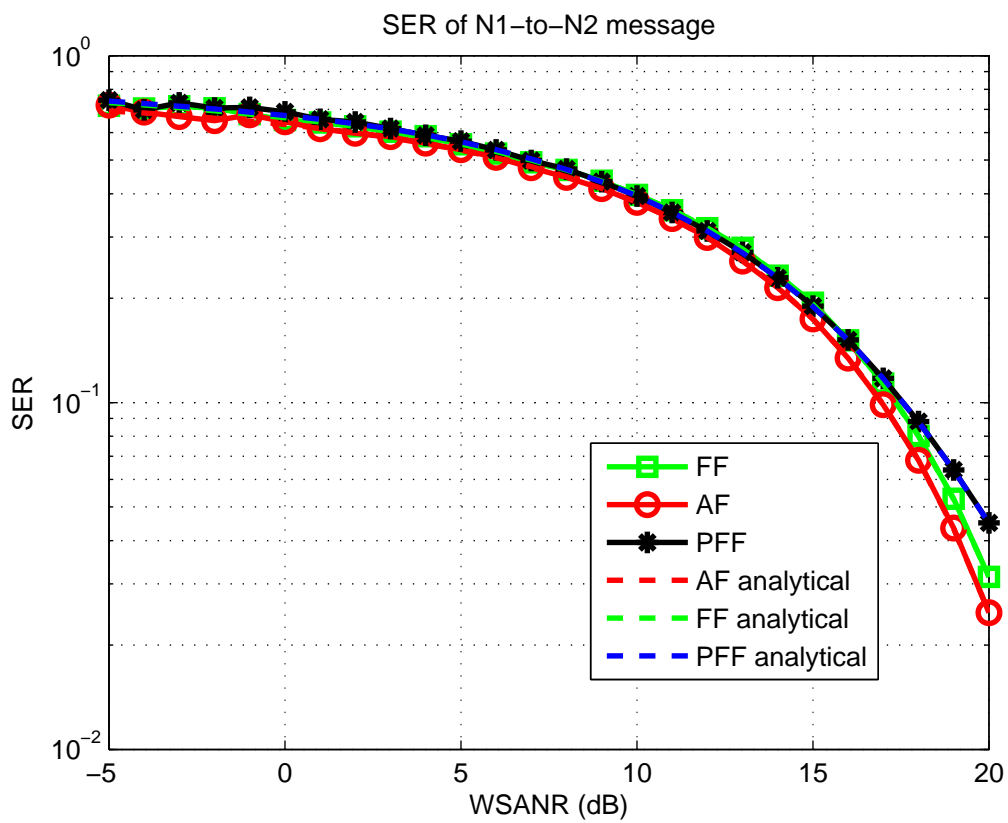


Figure 4.16: SER of T1 data of FF, AF and PFF systems when $h_1 = 1$ and $h_2 = 0.5$.

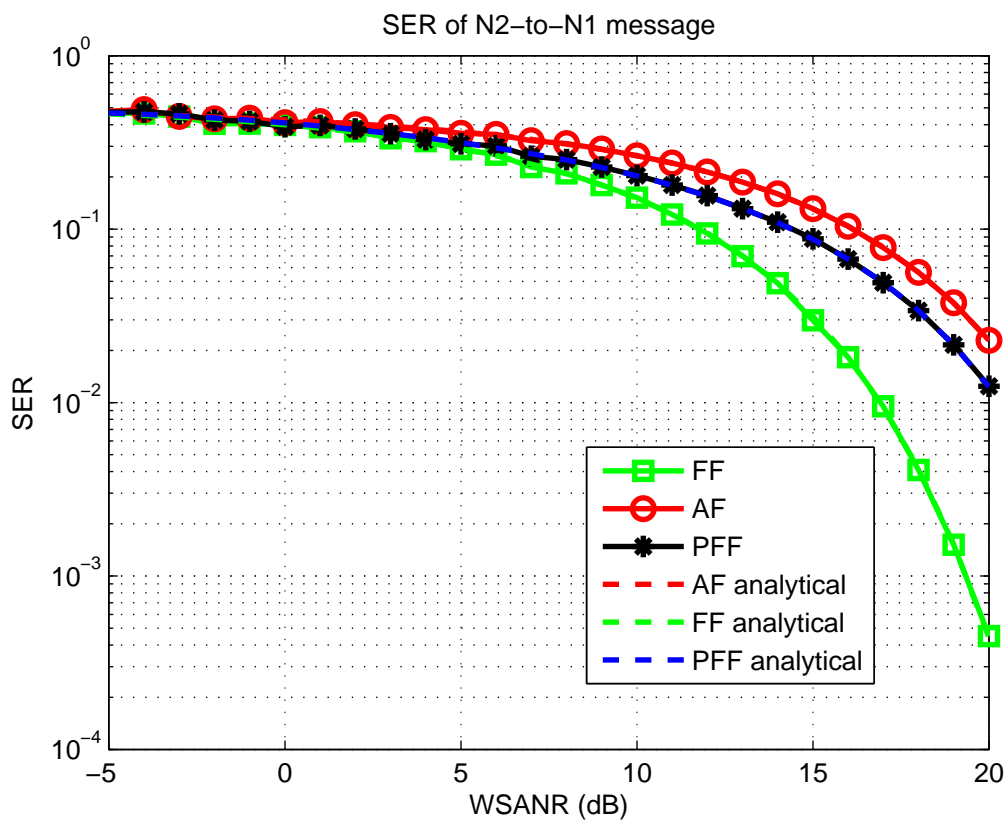


Figure 4.17: SER of T2 data of FF, AF and PFF systems when $h_1 = 1$ and $h_2 = 0.5$.

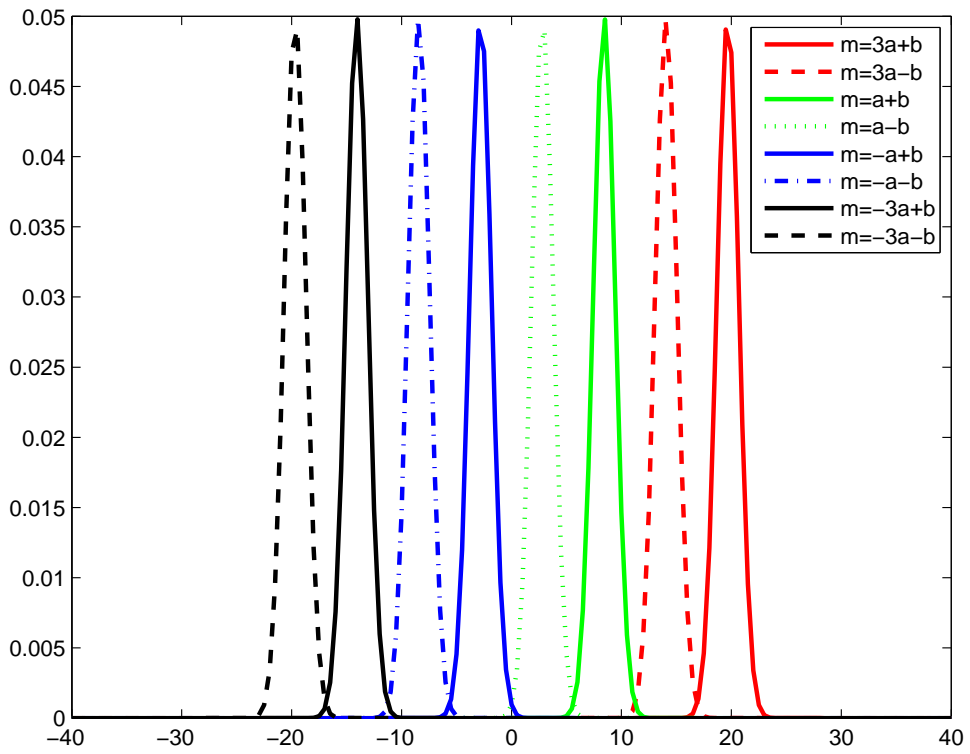


Figure 4.18: Signal distribution of Y_R when $h_1 = 1$ and $h_2 = 0.5$.

Chapter 5

Conclusion and Future Work

5.1 Conclusion

In this thesis, we first presented three transmission models of a relay system. The conventional relay transmission requires four time slots to complete one data exchange between two terminals. The network-coded relay transmission mixes the separately arrived data at the relay and broadcasts the result; it requires three time slots. The bidirectional relay transmission receives simultaneously arrived signal and then broadcasts the signal. It requires only two time slots to finish one data exchange between two terminals. We also introduced two classes of forwarding operation: amplify-and-forward (AF) and decode-and-forward (DF). An AF relay simply forwards the received signal with proper scaling, while DF relay decodes, re-encodes and then forwards the signal.

We mainly focused on a recently proposed AF-based forwarding strategy, which we termed fold-and-forward (FF). We discussed the FF operation, along with its power scaling and the detection rule. We also analyzed the symbol error performance using a two dimensional signal plane method. The simulation results showed that the performance gain of FF system depended on the channel condition and the terminals' modulation type. When the channels are strongly asymmetric, FF may not have better performance comparing to AF.

Thus, a bidirectional relay must select a proper forwarding strategy based on the channel condition.

5.2 Possible Future Work

Several possible extensions for our research are as follows:

- Employ fold-and-forward to MIMO relay systems.
- Consider joint design of forwarding strategy and the channel coding.
- Do channel estimation and analyze the impact of estimation error in bidirectional relay system.
- Consider design of forwarding strategy for two-dimensional signal constellations.



Bibliography

- [1] T. K.-Akino, P. Popovski, and V. Tarokh, “Optimized constellation for two-way wireless relaying with physical network coding,” *IEEE J. Sel. Areas Commun.*, vol. 27, no. 5, pp. 773–787, June 2009.
- [2] C.-B. Chae, T. Tang, R. W. Heath, Jr., and S. Cho, “MIMO relaying with linear processing for multiuser transmission in fixed relay networks,” *IEEE Tran. Signal Process.*, vol. 56, no. 2, pp. 727–738, Feb. 2008.
- [3] M. Chen and A. Yener, “Multiuser two-way relaying: detection and interference management strategies,” *IEEE Trans. Wireless. Commun.*, vol. 8, no. 8, pp. 4296–4305, Aug. 2009.
- [4] Y. Cheng, Y. Jiang, and X. You, “Preamble design and synchronization algorithm for cooperative relay systems,” in *Proc. IEEE Veh. Technol. Conf.-Fall*, Sep. 2009, pp. 1–5.
- [5] J. W. Craig, “A new simple and exact result for calculating the probability of error for two-dimensional signal constellations,” in *Proc. IEEE Military Commun. Conf.*, McLean, VA, Oct. 1991, pp. 571–575.
- [6] T. Cui, T. Ho, and J. Kliewer, “Memoryless relay strategies for two-way relay channels,” *IEEE Trans. Commun.*, vol. 57, no. 10, pp. 3132–3143, Oct. 2009.

- [7] C. Fragouli, J. Y. Boudec, and J. Widmer, “Network coding: an instant primer,” *ACM SIGCOMM Computer Communication Review*, vol. 36, no. 1, pp. 63–68, Jan. 2006.
- [8] F. Gao, T. Cui, and A. Nallanathan, “On channel estimation and optimal training design for amplify and forward relay networks,” *IEEE Trans. Wireless. Commun.*, vol. 7, no. 5, pp. 1907–1916, May 2008.
- [9] F. Gao, R. Zhang, and Y.-C. Liang, “Optimal channel estimation and training design for two-way relay networks,” *IEEE Trans. Commun.*, vol. 57, no. 10, pp. 3024–3033, Oct. 2009.
- [10] Y. Han, S. H. Ting, C. K. Ho, and W. H. Chin, “High rate two-way amplify-and-forward half-duplex relaying with OSTBC,” in *Proc. IEEE Veh. Technol. Conf.-Spring*, May 2008, pp. 2426–2430.
- [11] A. S. Ibrahim, A. K. Sadek, W. Su, and K. J. Ray Liu, “Coopertative communications with relay-selection: when to cooperate and whom to cooperate with?,” *IEEE Trans. Wireless. Commun.*, vol. 7, no. 7, pp. 2814–2827, July 2008.
- [12] Y. Jing and H. Jafarkhani, “Single and multiple relay selection schemes and their achievable diversity orders,” *IEEE Trans. Wireless. Commun.*, vol. 8, no. 3, pp. 1414–1423, March 2009.
- [13] S. Katti, H. Rahul, W. Hu, D. Katabi, M. Medard, and J. Crowcroft, “XORs in the air: practical wireless network coding,” *IEEE/ACM Trans. Networking*, vol. 16, no. 3, pp. 497–510, June 2008.
- [14] K. J. Ray Liu, A. K. Sadek, W. Su, and A. Kwasinski, *Cooperative Communications and Networking*. Cambridge University Press, 2009.

- [15] Y. Mei, Y. Hua, A. Swami, and B. Daneshrad, “Combating synchronization errors in cooperative relays,” in *Proc. IEEE Int. Conf. Acous. Speech Signal Process.*, vol. 3, March 2005, pp. iii/369–iii/372.
- [16] R. U. Nabar, H. Bolckei, and F. W. Kneubuhler, “Fading relay channels: performance limits and space-time signal design,” *IEEE J. Sel. Areas Commun.*, vol. 22, no. 6, pp. 1099–1109, Aug. 2004.
- [17] P. Popovski, and H. Yomo, “Physical network coding in two-way wireless relay channels,” in *Proc. IEEE Int. Conf. Commun.*, June 2007, pp. 707–712.
- [18] C. E. Shannon, “Two-way communication channels,” in *Proc. 4th Berkeley Symp. Math. Stat. Prob.*, 1961, pp. 611–644.
- [19] T. Unger and A. Klein, “Applying relay stations with multiple antennas in the one- and two-way relay channel,” in *IEEE Int. Symp. Personal Indoor Mobile Radio Communications*, Sep. 2007, pp. 1–5.
- [20] T. Wang and G. B. Giannakis, “Complex field network coding for multiuser cooperative communications,” *IEEE J. Sel. Areas Commun.*, vol. 26, no. 3, pp. 561–571, Apr. 2008.
- [21] J. Yu, D. Liu, C. Yin, and G. Yue, “Relay-assisted MIMO multiuser precoding in fixed relay networks,” in *Proc. Wireless Communications, Networking and Mobile Computing*, Sep. 2007, pp. 881–884.
- [22] M. Yu and J. Lin, “Is amplify-and-forward practically better than decode-and-forward or vice versa,” in *Proc. IEEE Int. Conf. Acous. Speech Signal Process.*, vol. 3, March 2005, pp. iii/365–iii/368.
- [23] S. Zhang, S. C. Liew, and P. P. Lam, “Hot topic: physical-layer network coding,” in *Proc. 12th Annual Int. Conf. Mobile Comput. Network. ACM*, pp. 358–365, 2006.

作者簡歷

學生盧世榮，民國七十五年九月出生於高雄市。民國九十七年六月畢業於國立交通大學電機資訊學士班，並於同年九月進入國立交通大學電子工程研究就讀，從事通訊系統方面相關研究。民國九十九年七月取得碩士學位，碩士論文題目為『無線雙向中繼傳輸之前送策略研究』。研究範圍與興趣包括：通訊系統、中繼傳輸、數位信號處理等。

